Received: 21 January 2022 | Revised: 14 March 2022 | Accepted: 24 March 2022

DOI: 10.1002/inf2.12318

REVIEW ARTICLE

WILEY

Thermally drawn multifunctional fibers: Toward the next generation of information technology

Yanan Shen[1,2,3] | **Zhe Wang**[4] | **Zhixun Wang**[4] | **Jiajia Wang**[5] | **Xiao Yang**[1,2] | **Xinghua Zheng**[1,3] | **Haisheng Chen**[1,2,3] | **Kaiwei Li**[6] | **Lei Wei**[4] | **Ting Zhang**[1,2,3,7]

[1]Institute of Engineering Thermophysics, Chinese Academy of Sciences, Beijing, China

[2]Nanjing Institute of Future Energy System, Nanjing, China

[3]University of Chinese Academy of Sciences, Beijing, China

[4]School of Electrical and Electronic Engineering, Nanyang Technological University, Singapore, Singapore

[5]College of Agricultural Equipment Engineering, Henan University of Science and Technology, Luoyang, China

[6]Key Laboratory of Bionic Engineering of Ministry of Education, Jilin University, Changchun, China

[7]Innovation Academy for Light-duty Gas Turbine, Chinese Academy of Sciences, Beijing, China

Correspondence

Kaiwei Li, Key Laboratory of Bionic Engineering of Ministry of Education, Jilin University, Changchun 130022, China.
Email: kaiwei_li@jlu.edu.cn

Lei Wei, School of Electrical and Electronic Engineering, Nanyang Technological University, 50 Nanyang Avenue, Singapore 639798, Singapore.
Email: wei.lei@ntu.edu.sg

Ting Zhang, Institute of Engineering Thermophysics, Chinese Academy of Sciences, Beijing 100190, China.
Email: zhangting@iet.cn

Funding information

A*STAR under AME IRG, Grant/Award Number: A2083c0062; Funding of Innovation Academy for Light-duty Gas Turbine, Chinese Academy of Sciences, Grant/Award Number: CXYJJ21-ZD-02; National Natural Science Foundation of China, Grant/Award Numbers: 51976215, 52172249, 62005101; Schaeffler Hub for Advanced Research at NTU, under the ASTAR IAF-ICP Programme, Grant/Award Number: ICP1900093; Scientific Instrument Developing Project of the Chinese Academy of Sciences, Grant/

Abstract

As the fundamental building block of optical fiber communication technology, thermally drawn optical fibers have fueled the development and prosperity of modern information society. However, the conventional step-index configured silica optical fibers have scarcely altered since their invention. In recent years, thermally drawn multifunctional fibers have emerged as a new yet promising route to enable unprecedented development in information technology. By adopting the well-developed preform-to-fiber manufacturing technique, a broad range of functional materials can be seamlessly integrated into a single fiber on a kilometer length scale to deliver sophisticated functions. Functions such as photodetection, imaging, acoustoelectric detection, chemical sensing, tactile sensing, biological probing, energy harvesting and storage, data storage, program operation, and information processing on fiber devices. In addition to the original light-guiding function, these flexible fibers can be woven into fabrics to achieve large-scale personal health monitoring and interpersonal communication. Thermally drawn multifunctional fibers have opened up a new stage for the next generation of information technology. This review article summarizes an overview of the basic concepts, fabrication processes, and developments of multifunctional fibers. It also highlights the significant progress and future development in information applications.

Award Number: YJKYYQ20200017; Singapore Ministry of Education Academic Research Fund Tier 1, Grant/Award Numbers: MOE2019-T1-001-103 (RG 73/19), MOE2019-T1-001-111 (RG 90/19); Singapore Ministry of Education Academic Research Fund Tier 2, Grant/Award Numbers: MOE-T2EP50120-0002, MOE2019-T2-2-127; Singapore National Research Foundation Competitive Research Program, Grant/Award Number: NRF-CRP18-2017-02; Nanyang Technological University

KEYWORDS

acoustoelectric fiber, biological probe, energy fiber, integrated circuit fiber, multifunctional fiber, optoelectronic fiber

1 | INTRODUCTION

The successful manufacture and employment of optical fibers have significantly improved the quality of human life in the last few decades.[1–4] As an essential platform for delivering numerous data, optical fibers have been utilized for thousands of meters of internet and telecommunications.[1,2,4,5] The applications of optical fibers are further extended to other fields, including medicine, sensing, and laser.[4] The inherent advantages of realizing these applications are attributed to the material properties and one-dimensional (1D) structure, including excellent optical transport performance with low loss, flexibility with proper bending, and long-distance transmission.[2,6] Generally, conventional optical fibers are produced from fused silica and depend on total internal reflection to transmit near-infrared light waves at 1.3 or 1.5 μm.[7,8] In the 1990s, an advanced low-loss dielectric waveguide called photonic crystal fibers was developed, which innovatively expanded the functions of optical fibers.[7,9] Inspired by the unique structures beyond conventional fibers, researchers have shown great interest in exploring advanced fiber-based electronics with multiple functionalities.[8] Compared with conventional electronic devices, fiber-based electronics possess individual characteristics, including high length-diameter ratio, excellent deformation ability, the feasibility of being woven into fabrics, light-weight, and wearability, which have a variety of unique application prospects.[10–15] The fabrication of fiber electronic devices integrates various materials (e.g., bulk polymers, glasses, metals, semiconductors, and nanomaterials), enabling various sophisticated functions in the fiber platform.[14–17] Therefore, significant efforts have been made to explore those fibers with abundant functions, such as implantable biomedical probes or scaffolds,[18] thermal and pressure detection,[15,19–21] chemical identification,[22,23] medical health monitoring,[24–26] soft batteries or super capacitors,[27–29] energy generators,[30–32] and so on.[5,16,33–35]

Nevertheless, due to the prescribed geometry and the difference of properties and interface combination between functional materials, there are limitations in the initial construction of multi-material systems.[2,3,11] Some nano-scale devices have been prepared using various wafer-based methods, but they are presented in planar geometries and sophisticated steps.[3,17,36] Moreover, several different fiber fabrication strategies have been developed, including solution-based methods, dry fabrication methods, and spinning processes.[37] However, the dry fabrication methods (e.g., physical vapor deposition[38] and chemical vapor deposition[39,40]) require a vacuum and high-temperature conditions. Besides, solution-based methods (e.g., dip coating[41,42] and printing[43,44]) and spinning processes (e.g., electrospinning[45,46] and wet-spinning[47,48]) are restricted due to the difficulty of large-scale fabrication and the lack of potential for designing complex architectures.[11,13,49] At present, the related technology of the thermal drawing method to produce the traditional optical fibers has been widely used in industrial manufacturing. The set of fabrication has successfully achieved integrating various functional materials into fibers to form structures at micro- and nano-scale, which provides a possibility for efficient preparation of flexible electronic devices.[50]

Compared with other fiber fabrication strategies, the thermal drawing method demonstrates unique advantages of customizable structure, large-scale manufacturing, and easy combination with other techniques.[17,51] The thermal drawing process starts from preform fabrication with a macroscopic size, which reduces the difficulty of incorporating functionalities and constructing particular geometries.[52] Then, the designed preform with a length of tens of centimeters to meters is heated in the furnace of the drawing tower and drawn into kilometers-long fibers by regulating the relationship between viscous force, internal stress, and surface tension.[52] More recently, the thermal drawing method has shown excellent technical compatibility, which is reported to be combined with laser treatment,[53–57] three-dimensional (3D) printing approach,[54,58] ultraviolet exposure method,[59] sonochemical treatment,[35] direct imprinting

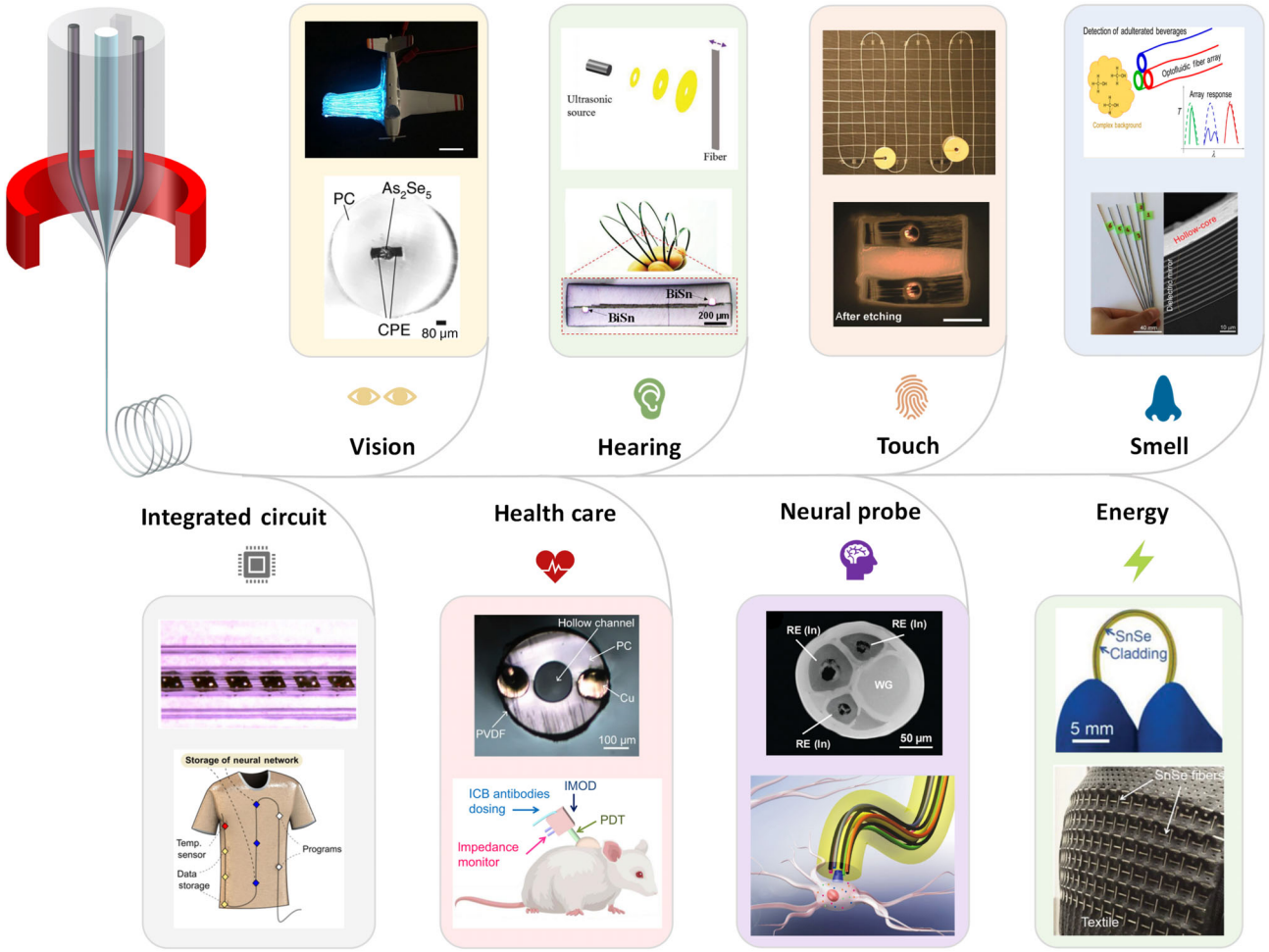

FIGURE 1 Classifications of thermally drawn functional fibers applied to information technology. Thermal drawing process; Visual functional fiber. Reproduced with permission.[54] Copyright 2019, Springer Nature; Auditory functional fiber. Reproduced with permission.[60] Copyright 2017, WILEY-VCH; Tactile functional fiber. Reproduced with permission.[15] Copyright 2020, WILEY-VCH; Olfactory functional fiber. Reproduced with permission.[61] Copyright 2013, American Chemical Society. Reproduced with permission.[62] Copyright 2016, The Optical Society; Integrated circuit fiber. Reproduced with permission.[63] Copyright 2021, Springer Nature; Biochemical probe fiber. Reproduced with permission.[64] Copyright 2021, Springer Nature; Neural probe fiber. Reproduced with permission.[65] Copyright 2021, Wiley-VCH; Energy fiber. Reproduced with permission.[53] Copyright 2020, WILEY-VCH

technique,[51] and the photolithography process.[14,52] For example, the laser treatment can not only recrystallize the polycrystalline SnSe core to obtain single-crystal SnSe fibers, but also manufacture micro/nanoparticles via Rayleigh–Plateau instability caused by laser heating.[53–57] Combining the advanced techniques with thermally drawn fibers provides more application scenarios, including vision, hearing, touch, smell, energy, neural probe, biochemical probe fiber, and integrated circuit fiber, as described in Figure 1.

The next generation of information technology mainly includes big data, cloud computing, the internet of things, artificial intelligence, and human-computer interaction. In fact, digital information acquisition technology based on natural motion perception and wearable electronic terminals is leading a new round revolution in internet of things, artificial intelligence, and human-computer interaction. Thermally drawn fibers play a prominent role in flexible information collection, wearable devices power supply, and integration of different sensors or electric devices on the same platform (chemistry, physics, optics, and electricity). As a result, these fibers will become one of the driving forces behind the next generation of information technology. The scope of this review will focus on novel multifunction fibers for information communication and look forward to providing more valuable references for the information technology revolution. This article reviews several methodologies according to their different functions and applications, including vision, hearing, touch, smell, and other

information applications. This article introduces the significant processes and the development of thermally drawn fibers. In addition, the fabrications, structures, and properties of the thermally drawn fiber-based devices are comprehensively summarized. Finally, the future research directions of the thermally drawn fiber are discussed.

2 | THERMAL DRAWING PROCESS

Nowadays, the internet and most telecommunications transmit information by using optical fibers as a medium to deliver light waves and send enormous amounts of data around the world.[1] Generally, most optical fibers are fabricated through the thermal drawing process. The thermal drawing process involves heating the preform above the softening temperature and stretching the preform into kilometers of fibers in a viscous state.[17,66] Similarly, using the same principle, materials with optical, electronic, photoelectric, and thermal properties are combined to fabricate multimaterial composite fibers.[2,17] In the process of stretching, the multimaterial macroscopic preform is placed in the furnace with one end fixed on the top of the drawing tower. The other end is softened or melted when the temperature exceeds the glass transition temperature. After a period of heating, the fiber is drawn from the softened preform and undergoes necking to a controllable diameter fiber under the external force of turning capstans. The diameter of the fiber D_{fiber} is regulated by controlling the drawing temperature T_{draw} of the hottest area in the furnace, the feeding speed v_{feed} of the preform, and the drawing speed v_{draw} of the blank.[2,11,66] Ignoring the expansion of materials, the diameter of the fiber D_{fiber} is a function of the diameter of the preform D_{preform}, and is related to the feeding speed v_{feed}, and the drawing speed v_{draw}, according to the volume conservation $D_{\text{fiber}} = D_{\text{preform}}\sqrt{\frac{v_{\text{feed}}}{v_{\text{draw}}}}$. In this process, it is noted that the preform can be fabricated in many approaches, such as rod-in tube approach,[67,68] extrusion,[69,70] the stack and draw, thin-film rolling technology, 3D printing technology,[71–73] melt-casting process,[74] and double-crucible approach.[75]

As a multimaterial top-down process, multimaterial thermal drawing embodies several distinct advantages. The final manufactured fiber has a similar geometry, composition, and cross-section as the preform, but it is just a miniature version of the preform during thermal drawing. Due to the macroscopic size of the preform, a sophisticated transverse cross-section with various structures and multiple materials can be achieved.[1,66,76,77] In addition, the preform integrates a wealth of functionalities, including optical sensing, energy storage, ion movement detection,[5] chemical sensing, sports performance monitoring,[5] leading aboard application prospects in soft electronics with the consideration of the advantages of nanometer feature sizes, high integration, and stretchability.[5] Besides, from the industrialization perspective, thermal drawing is an automatic process in which the preform is drawn into fibers with accurate control of size and axial uniformity. Compared with other fibers preparation methods, kilometers of fibers can be fabricated on a large scale.[1,66] Furthermore, the functional material in the core is encapsulated with cladding, which can avoid leakage of harmful substances and protect the functional material from the intrusion of water and air. Thus, the thermally drawn fiber is washable and resistant to perspiration impregnation.[66]

However, due to the differences in thermal, mechanical, and chemical properties of different materials, the integration of various materials faces challenges. To solve these problems, there are specific guidelines on material selections to ensure that diverse materials can be drawn together from the preform while maintaining the complex transverse structure during the drawing process.[36,76]

1. The material of cladding and core should be chosen to have a similar melting temperature or glass transition temperature. However, the drawing temperature must be higher than the melting temperature or glass transition temperature and lower than the boiling temperature.[1,36,76]
2. The thermally drawn fiber should have at least one amorphous material that can support the fiber structure and achieve continuous and controllable deformation from the preform to the fiber in the necking process.[1,3,36]
3. Materials should exhibit good adhesion/wettability in viscous and solid-state and will not crack even after rapid thermal cooling and quenching.[3,17,76]
4. The thermal properties of the materials should be relatively similar, including thermal expansion properties and viscosity, which can avoid undesirable breakages and cracks caused by thermomechanical mismatches.[1,36]

Generally, thermally drawn multimaterial fibers can be divided into three types depending on their structures and forming process. The first type of multimaterial thermally drawn fiber was first invented in 2002. It is drawn directly from the preform without postprocess and maintains a continuous and constant component. In the case of the first fiber, only a physical shrinkage of the inner core occurs during the thermal drawing process.[56] The second type of fiber is characterized by an asymmetrical structure, in which the cross-section of the fiber is

different throughout the fiber length.[2,78–82] When a heat source is applied to the fiber at a specific temperature, the cladding material softens, and the core becomes a flowing state. Under the force of the surface tension and viscous, the fluid core tends to break up and split into spherical droplets, which is called Plateau–Rayleigh capillary instability.[1,2,36] The chemical interaction characterizes the third type of fibers during the drawing process. When the preform is heated in the furnace, the composition of the material in the preform undergoes a chemical process to form new compounds in the fiber.[83,84]

3 | OPTOELECTRONIC FIBERS

The optoelectronic fibers that possess the primary function of photoelectric response involve incorporating

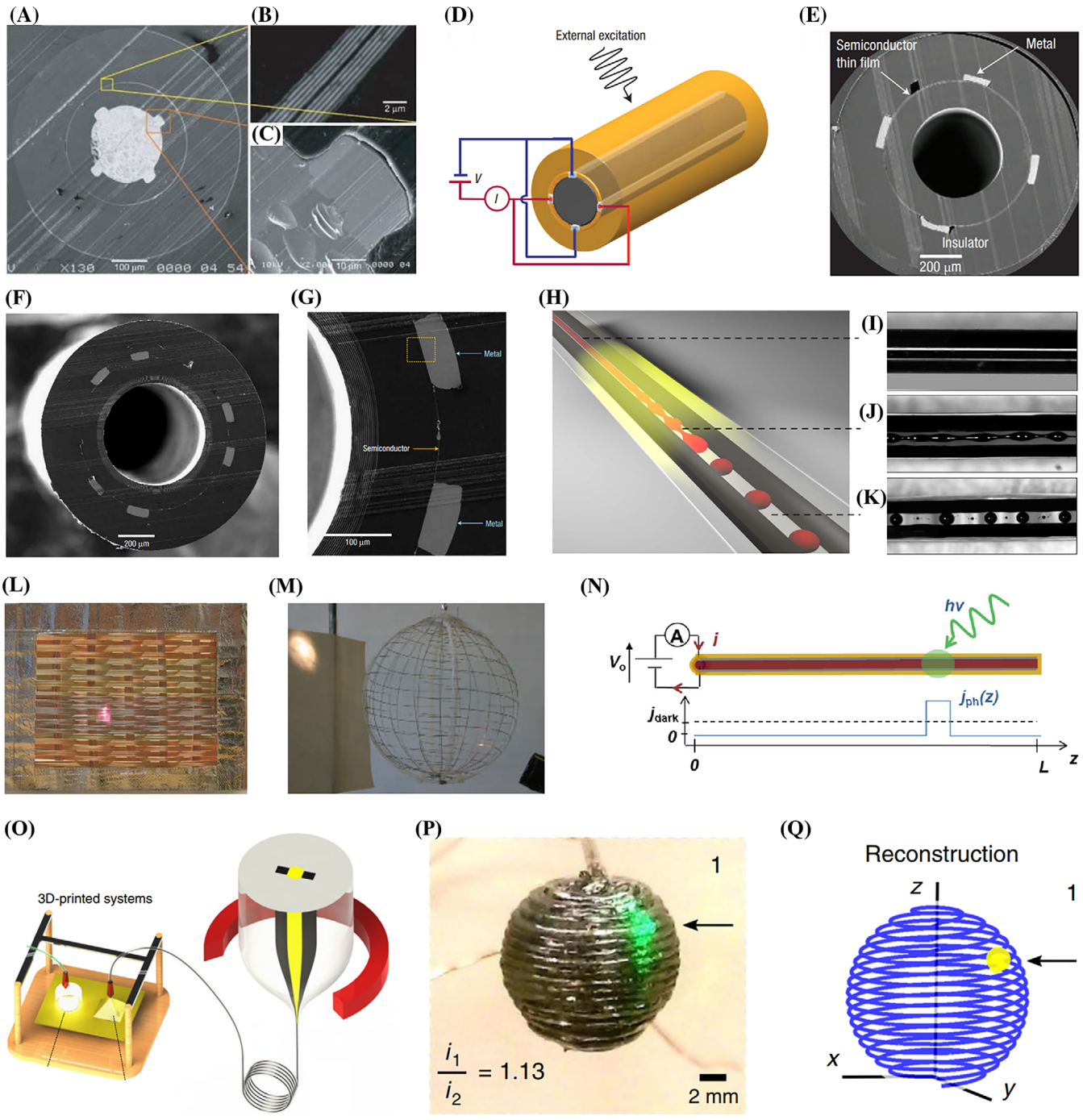

FIGURE 2 Legend on next page.

semiconducting, conducting, and insulating materials inside a 1D single fiber with a designed electrical conducting configuration.[3] They can be fabricated using the preform-to-fiber thermal drawing technique on a kilometer-scale with high uniformity and low cost. Compared to the traditional optoelectronic devices manufactured by the standard semiconductor manufacturing process, the optoelectronic fibers are soft, flexible, and can easily be woven into fabric or printed into a desired 3D architecture. In this section, we review the development of optoelectronic fibers, emphasizing their fabrication and applications across the field of photodetection and optical imaging.

3.1 | Photodetection fibers

To obtain the primary metal–semiconductor–insulator construct in a thermally drawn fiber, the metallic electrodes and the semiconductor core, embraced by transparent cladding in the preform, are specifically precisely designed to form intimate electrical contact during the thermal drawing process. The thermal processing property of these different functional materials should match well so as to realize co-drawing. The electrode can be made of metals Sn, In, and low melting-point metallic alloys for polymer matrices fibers and Pt for silica matrices fibers. For the semiconductor core, chalcogenide glasses with outstanding photoelectric performance are usually adopted for polymer matrices fibers, and Si, Ge, and Si—Ge compound for silica matrices fibers.

The first optoelectronic fiber was demonstrated by Bayindir et al. in 2004.[85] As shown in Figure 2A–C, the fiber consists of a 200-μm chalcogenide glass ($As_{10}Se_{50}Te_{10}Sn_5$) core, two pairs of Sn metal electrodes that are in close contact with the core, an optical resonant cavity that encircles the core and electrodes, and a polyethersulphone (PES) cladding. When external light with a wavelength match with the transmission band of the optical resonant cavity illuminates the fiber, the photocurrent raises immediately owing to the photoconductive effect (Figure 2D).[86] However, due to the bulky size of the semiconductor core, the photogenerated carriers and holes recombine quickly and lead to an increased noise level, degrading the fiber's performance. As a result, the photoelectric conversion efficiency remains low compared with the commercialized Si-based photodetector. Later studies by Sorin et al. revealed that by decreasing the fiber photodetector's diameter, the noise level could be effectively suppressed, and the sensitivity increases linearly. They also proposed a new design of fiber photodetector with thin semiconductor nanofilms embedded inside the fiber along the fiber length (Figure 2E). They achieved an increased sensitivity with more than an order of magnitude higher than the bulky semiconductor core device.[87] Alternatively, the photoelectric detection function can also be realized in multi-material fibers utilizing the photothermal effect. Bayindir et al. reported an optoelectronic fiber design that can transmit high power mid-infrared laser and detect localized defect formation along the fiber simultaneously.[88] The cross-section image of the fiber is displayed in Figure 2F,G. A central hole enclosed by a 1D circular photonic bandgap (PBG) structure serves as the path for light guidance. A thermal sensitive semiconductor ($Ge_{15}As_{25}Se_{15}Te_{45}$; GAST) thin layer and multiple electrodes are buried in the PES cladding to

FIGURE 2 Photodetection fibers. (A) SEM micrograph of the cross-section of an optoelectronic fiber with a 200-μm chalcogenide glass core surrounded by electrodes, a resonant cavity, and polyethersulphone (PES) cladding. Reproduced with permission.[85] Copyright 2004, Springer Nature. (B) A magnified image of the resonant optical cavity structure. Reproduced with permission.[85] Copyright 2004, Springer Nature. (C) A magnified micrograph of the semiconductor–metal interface. Reproduced with permission.[85] Copyright 2004, Springer Nature. (D) A schematic diagram of the fiber photodetector. Reproduced with permission.[86] Copyright 2006, WILEY-VCH; (E) SEM micrograph of the cross-section of a thin semiconductor film optoelectronic fiber. Reproduced with permission.[87] Copyright 2007, WILEY-VCH. (F) The cross-section of a photothermal effect-based optoelectronic fiber with a hollow-core 1D PBG structure, heat-sensitive layer, metallic conduits, and protective polymer cladding. Reproduced with permission.[88] Copyright 2005, Springer Nature. (G) Enlarged view of the PBG structure and the optoelectronic device. Reproduced with permission.[88] Copyright 2005, Springer Nature. (H) Illustration of the selective breakup process. Reproduced with permission.[81] Copyright 2016, Springer Nature. (I–K) Optical micrograph of a multimaterial fiber before the breakup, during the onset of breakup process, and after the breakup, respectively. Reproduced with permission.[81] Copyright 2016, Springer Nature. (L) A woven 2D photodetecting fiber web. Reproduced with permission.[85] Copyright 2004, Springer Nature. (M) A closed spherical photodetecting fiber web. Reproduced with permission.[89] Copyright 2006, Springer Nature. (N) Schematic of a connected photodetecting fiber with an illumination event. Reproduced with permission.[90] Copyright 2010, Optical Society of America. (O) Schematic of the modified 3D printing using the multimaterial fiber. Reproduced with permission.[54] Copyright 2019, Springer Nature. (P) A 3D printed sphere from optoelectronic fibers illuminated by a laser beam. Reproduced with permission.[54] Copyright 2019, Springer Nature. (Q) Exacted imaging and reconstruction of the laser spots. Reproduced with permission.[54] Copyright 2019, Springer Nature

form the photodetecting device. The light leaking through local defect heats the fiber locally and decreases the resistance of the semiconductor layer. Another clever design was introduced by Rein et al., which was realized by the selective breakup of the semiconductor core to build contact between the semiconductor spheres and the electrodes.[80,91] As shown in Figure 2H–K, the semiconductor core and the electrode of the thermally drawn fiber are deliberately designed to be separated by a small gap all along the fiber.[81] Post heating treatment is to heat the semiconductor core above its softening temperature or melting temperature, and the core breaks into separate spheres with enlarged diameter and forms contact between the sphere and the electrodes spontaneously.

The flexible photodetection fibers can be woven into a two-dimensional (2D) photodetector fabric with $N \times N$ pixels. As shown in Figure 2L, the photodetector array can be used to localize an illumination point on the surface.[85] Moreover, by constructing the photodetection fiber into a spherical web, the direction of the incident beam can be readily obtained via localizing the incident point and the exit point (Figure 2M).[89] Although a 2D photodetection fiber array can perceive a beam's position, the extraction of spatially resolved illumination along a single fiber seemed fundamentally challenging. Sorin et al. developed an approach that broke the axial symmetry by constructing a convex electrical potential along the fiber axis and reconstructing an arbitrary rectangular optical wave profile (Figure 2N).[90] The optoelectronic filaments can be printed into a 3D shape using a modified 3D printing technique with the inner structure retained, realizing light impingement point localization across the entire fiber length (Figure 2O–Q).[54]

3.2 | Optoelectronic fibers for optical imaging

An advanced function of the optoelectronic fiber is optical imaging, which can further extend its applications in various fields. To render the photodetection fiber or devices made from the fiber to see the 2D picture, complex fiber structures, special strategies, and reconstruction algorithms are required. Abouraddy et al. demonstrated the first fiber web-based optical imaging device (Figure 3A,B) by adapting the computerized axial tomography (CAT) strategy, which is commonly used in x-ray imaging of 3D bodily structures.[89] Although each fiber element can only record the line integral of the intensity distribution of the optical field along its length, by rotating the imaging fiber web or the object that is being imaged, adequate information can be obtained, and the image can be reconstructed using a tomographic algorithm (Figure 3C). Aside from the field distribution, the phase distribution can also be imaged by introducing an additional fiber imaging web. Sorin et al. developed a dual ring in-fiber photodetection architecture which is capable of wavelength discrimination in the visible range with high resolution and demonstrated imaging with polychromatic illumination using a single fiber web (Figure 3D,E).[6] Another route to construct optical imaging devices is to combine thermally drawn semiconductor nanowires arrays with lithographically defined electrode arrays (Figure 3F,G).[92] Each light-responsive pixel is formed by contacting the parallel semiconductor nanowires between two electrodes. Alphabetic characters can be identified with high fidelity using the pixel array (Figure 3H,I). Although various optoelectronic fiber-based imaging devices have been proposed and demonstrated, the semiconductor core drawn directly remains amorphous, and the photodetection performances are far below the commercialized imaging devices. Yan et al. developed a sonochemical post-treatment strategy to grow semiconductor nanowires out of the amorphous core (Figure 3J,K).[35] Unprecedented performance was achieved using the semiconducting nanowire embedded optoelectronic fiber, and fluorescent imaging was demonstrated in Figure 3L–N.

4 | ACOUSTOELECTRIC FIBERS

Creating fibers comprised of conductors and piezoelectric materials allows for the realization of acoustoelectric fiber devices. This section summarizes the fabrication details and applications of thermally drawn acoustoelectric fibers.

It is essential to form a structure of piezoelectric materials with electrically conductive domains within the drawn fibers in order to make acoustoelectric fibers. Since the cladding materials are usually thermoplastics, they offer better mechanical performance than glasses. Generally, the drawing temperature of these fibers is relatively low, typically in the range of 200–400°C. Low melting point metals like tin, bismuth, indium, and their alloys, and conductive thermoplastics like carbon-loaded polyethylene (CPE) and carbon-loaded polycarbonate (CPC) are conductors that are compatible with this process. Similar requirements also apply to the selection of piezoelectric materials. The piezoelectric material used in the thermal drawing should be drawable, thermally, and chemically stable during the process. Poly(vinylidene fluoride) (PVDF), its copolymers such as poly(vinylidene fluoride trifluoroethylene) (P(VDF-TrFE)) and PVDF-based composites with high melting point inorganic piezoelectric materials are excellent materials for thermally drawn acoustoelectric fibers as a highly nonreactive thermoplastic piezoelectric material.

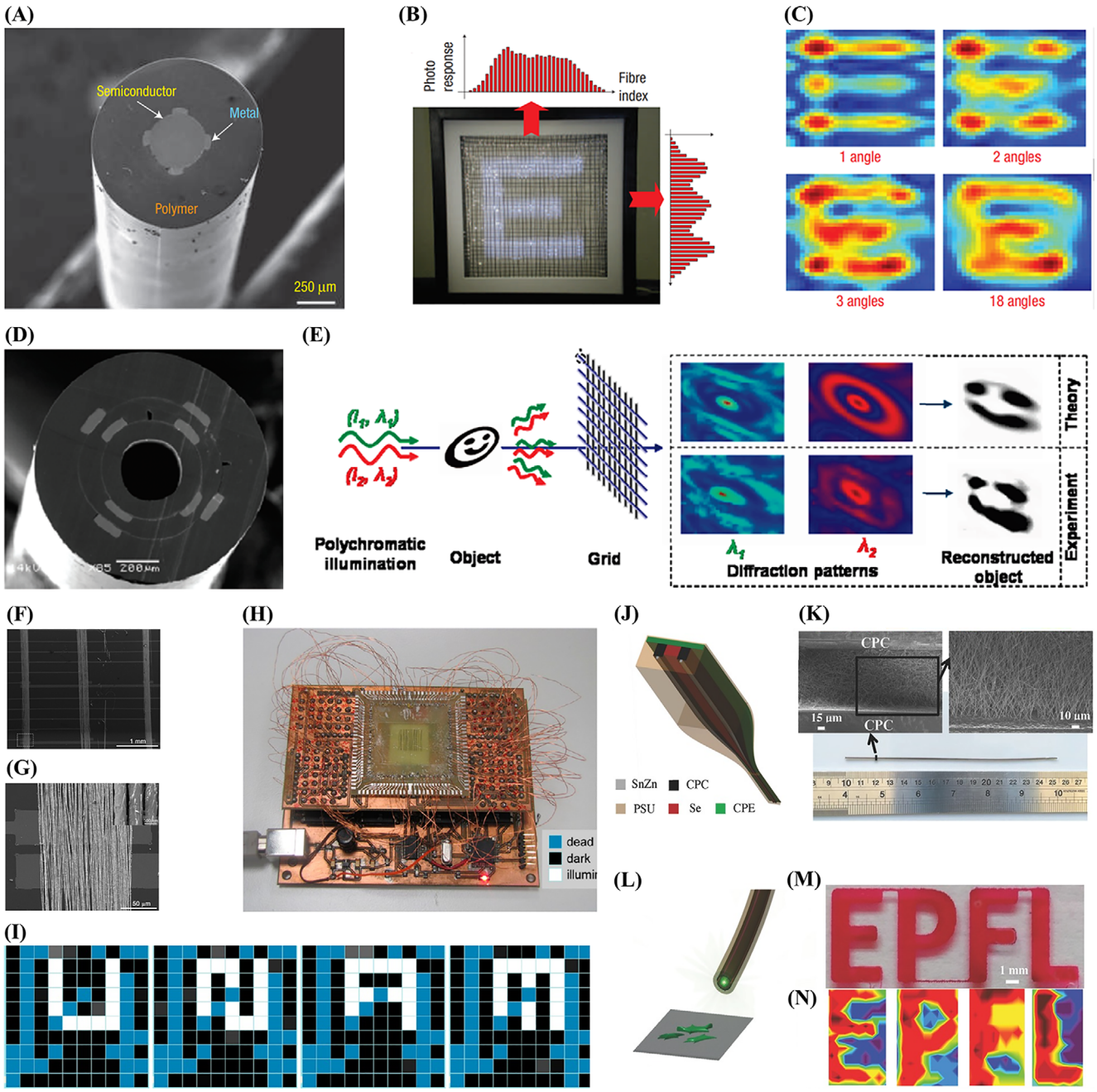

FIGURE 3 Optoelectronic fibers for optical imaging. (A) SEM image of the cross-section of an optoelectronic fiber. Reproduced with permission.[89] Copyright 2006, Springer Nature. (B) A 2D imagining web illuminated by an E-shaped light beam. Reproduced with permission.[89] Copyright 2006, Springer Nature. (C) Reconstructed image of the light beam with different incident angles. Reproduced with permission.[89] Copyright 2006, Springer Nature. (D) SEM micrograph of a dual-ring optoelectronic fiber. Reproduced with permission [6] Copyright 2009, American Chemical Society. (E) Principle of single grid lensless polychromatic imaging. Reproduced with permission.[6] Copyright 2009, American Chemical Society. (F) SEM image of the nanowires over electrical contacts. Reproduced with permission.[92] Copyright 2012, American Chemical Society. (G) A magnified image of a photoconductive pixel with hundreds of nanowires. Reproduced with permission.[92] Copyright 2012, American Chemical Society. (H) Macroscopic nanowire photo imaging device. Reproduced with permission.[92] Copyright 2012, American Chemical Society. (I) The captured alphabetic characters of "UNAM" by the device. Reproduced with permission.[92] Copyright 2012, American Chemical Society. (J) Schematic of the thermal drawing of fiber for growing Se nanowires along the fiber length. Reproduced with permission.[35] Copyright 2017, John Wiley and Sons. (K) Photograph of a 15 cm fiber and SEM images showing the Se nanowire mesh and its interface with a CPC electrode. Reproduced with permission.[35] Copyright 2017, John Wiley and Sons. (L) Schematic of the fluorescence imaging system. Reproduced with permission.[35] Copyright 2017, John Wiley and Sons. (M) Photograph of the "EPFL" logo filled with dye Rhodamine B dissolved in ethanol. Reproduced with permission.[35] Copyright 2017, John Wiley and Sons. (N) Fluorescent image obtained with the hybrid fiber device. Reproduced with permission.[35] Copyright 2017, John Wiley and Sons

The first acoustoelectric fiber prepared by thermal drawing was reported in 2010.[93] In the study, two types of acoustoelectric fiber are demonstrated. One has a lamellar structure, while the other has a concentric system, as shown in Figure 4A–C. Figure 4A illustrates the fabrication process of the preform for drawing the lamellar fiber. Two slabs of CPC sandwich a slab of P(VDF-TrFE), and an indium rod is placed along with each CPC slab. The whole structure is wrapped by two polycarbonate (PC) slabs. After consolidation, the macroscopic preform is thermally drawn into fibers that maintain the same structure but with reduced sizes of a few hundreds of microns (Figure 4B). A similar process is applied to the fabrication of cylindrical fiber, and Figure 4C shows the cross-section of the resulting cylindrical fiber. The two types of fibers have identical materials despite the different structures. The fibers can be used both as an acoustic sensor and as an acoustic actuator and are able to function underwater since the function part is encapsulated in insulating PC cladding. A schematic of the testing setup is shown in

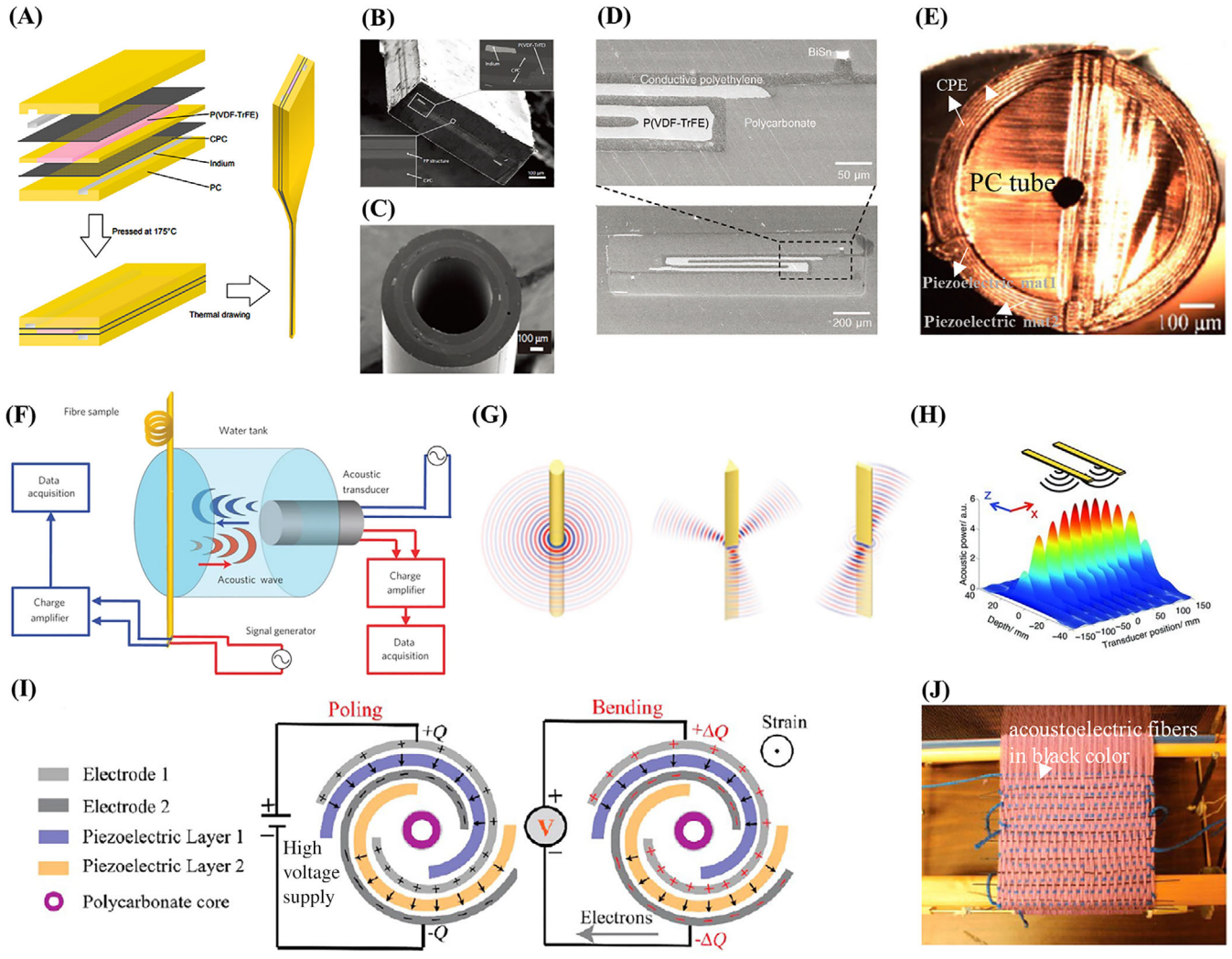

FIGURE 4 Thermally drawn acoustoelectric fibers: fabrication, structure, performance, and weavability. (A) A typical fabrication process of preforms. Reproduced with permission.[93] Copyright 2010, Springer Nature (B) Lamellar-structured fiber. Reproduced with permission.[93] Copyright 2010, Springer Nature. (C) Cylindrical fiber. Reproduced with permission.[93] Copyright 2010, Springer Nature. (D) Fiber with a large-active-area design. Reproduced with permission.[94] Copyright 2012, John Wiley and Sons. (E) Jelly roll fiber. Reproduced with permission.[95] Copyright 2017, American Chemical Society. (F) Underwater testing set-up. Reproduced with permission.[93] Copyright 2010, Springer Nature. (G) Acoustic wavefront from different fiber shapes. Reproduced with permission.[93] Copyright 2010, Springer Nature. (H) In-phase interference of two high-output acoustoelectric fibers. Reproduced with permission.[94] Copyright 2012, John Wiley and Sons. (I) Charge separation mechanism of the jelly roll fiber. Reproduced with permission.[95] Copyright 2017, American Chemical Society. (J) Acoustoelectric fiber textile. Reproduced with permission.[95] Copyright 2017, American Chemical Society

Figure 4F.[93] The fiber sample is coupled to a transducer across the water tank, with a signal generator and proper data acquisition system, the performance of the acoustoelectric fibers can be characterized. The acoustic wavefront and its associated radiation pattern from the fiber can be modified by designing the fiber shape. The finite-element calculation result of the acoustic wavefront emitting from the cylindrical, triangle, and rectangular fibers are shown in Figure 4G. Further, a Fabry–Perot optical cavity structure can be coupled to extend the potential applications of the acoustoelectric fiber in modulating sophisticated optical devices.

Acoustoelectric fibers with one thin piezoelectric material layer have a small active area and limited performance.[60,93] Chocat et al. introduced a large-active-area design in thermally-drawn acoustoelectric fiber.[94] As shown in Figure 4D, the fiber consists of P(VDF-TrFE) as the active part, CPE, and BiSn alloy as current buses. The fiber has a symmetrical structure in cross-section. The thick P(VDF-TrFE) layer is divided into three regions by the surrounding and inserted CPE layers. Those CPE layers have high viscosity during the drawing and function as support for the low viscosity P(VDF-TrFE), thus preventing the fiber structure from evolving toward an unfavored shape. The large-active-area design enhances the performance of the resulting acoustoelectric fiber, and Figure 4H shows the acoustic power generated by the in-phase interference of two resulting fibers.

An alternative design for acoustoelectric fiber is the jelly roll structure.[95] The fiber is comprised of multiple layers of conductors and piezoelectric materials, in the alignment of one conductor layer, piezoelectric material one, another conductor layer, piezoelectric material two, and repeating, as shown in Figure 4E. In this design, CPE is used as conductors, $BaTiO_3$ nanowires-P(VDF-TrFE), $Pb(Zr_{0.52}Ti_{0.48})O_3$ nanowires-P(VDF-TrFE), and carbon nanotubes-P(VDF-TrFE) composites are selected as active materials. This unique structure brings the jelly roll fiber with charge separation property, as shown in Figure 4I. The charge separation mechanism can be explained as the remained polarization from aligned dipoles formed via poling changes by the induced strain at fiber bending, and free charges in electrodes are forced to balance it. Aside from being used for sound detection, the jelly roll acoustoelectric fibers can be woven into a textile using a Dobby loom and lead to textile-based piezoelectric generators (Figure 4J).

5 | MULTIFUNCTIONAL FIBERS FOR CHEMICAL SENSING

Multimaterial fiber provides a versatile platform for chemical sensing. The hollow waveguide can serve as a path for the light signal and provide a microchannel to host the gaseous or liquid sample to analyze.[61,62,96,97] The built-in electrode makes the fiber a promising candidate for electrochemical analysis. More importantly, integrating photodetection devices inside the fiber eliminates the need for external detectors and provides the potential for distributed chemical sensing.[98]

5.1 | Optoelectronic chemical sensing

The optoelectronic nose (Figure 5A,B) is an early example of a multimaterial fiber chemical sensor that relies on the specific infrared absorption caused by the vibration or rotation of a chemical group.[99] The hollow PBG fiber formed by repeated As_2Se_3 and PES nanolayers (Figure 5C) plays a critical role in this sensor configuration because it can be used as an optical waveguide, wavelength selector, and gas cell simultaneously. The presence and level of infrared absorbing molecules in the channel can be inferred by the wavelength and loss of the transmitted signal (Figure 5C).[100] To realize multi-analytes discrimination and quantification, PBG fiber arrays with different transmission bands were developed (Figure 5D). The optoelectronic nose could find wide applications in the fields of food quality control, environmental monitoring, and breath analysis for disease diagnostics.

Another example is the chemiluminescence-based optoelectronic fiber chemical sensor. Figure 5E,F shows that the fiber was produced through the stacking and drawing method.[101] The fiber consists of a rectangular hollow core and two photodetection devices. The channel is designed to infiltrate the target peroxide vapor. The inner wall of the channel was modified with a specific chemiluminescent material that emits light when in contact with peroxide. The in-fiber photodetection devices can detect the emitted light and conceive the concentration. As the photodetection devices run all along the fiber length, distributed chemical sensing can be potentially realized (Figure 5G).

5.2 | Electrochemical sensing

Richard et al. proposed the first fiber integrated electrochemical devices by tailoring the fiber microstructure.[98] The fiber configuration is depicted in Figure 6A,B. It introduces two CPC electrodes that function as the working electrode and control electrode, respectively, a working electrode made of $Pt_{57.5}Cu_{14.7}Ni_{5.3}P_{22.5}$ (Pt-MG) and a liquid channel into a single fiber. The capability of such fiber to directly detect and quantify paracetamol was demonstrated by performing cyclic voltammetry and chronoamperometry (Figure 6C).

Moreover, an "electrochemical pipet tip" for direct sampling and analysis of microliter-range volumes was demonstrated (Figure 6D). Recently, Iwama et al. developed an electrochemical imaging system using a multi-electrode fiber. Figure 6E shows that the fiber contains 104 separated electrodes.[97] The fiber was placed in a bipolar electrochemical system that had a sample chamber containing potassium ferricyanide solution and a detection chamber containing [Ru(bpy)3]Cl2/tripropylamine (TPA) luminophore solution for measurement (Figure 6F). The charge-coupled device (CCD) camera can measure the electrochemiluminescence signal intensity pattern from those electrodes (Figure 6G). The tiny multi-electrode probe will be used in life science to image chemical dynamics within biological samples such as tissues and cells.

6 | THERMALLY DRAWN FIBERS FOR TACTILE SENSING

Tactile sensing is indispensable for the next generation of information devices to "feel" the external physical stimuli

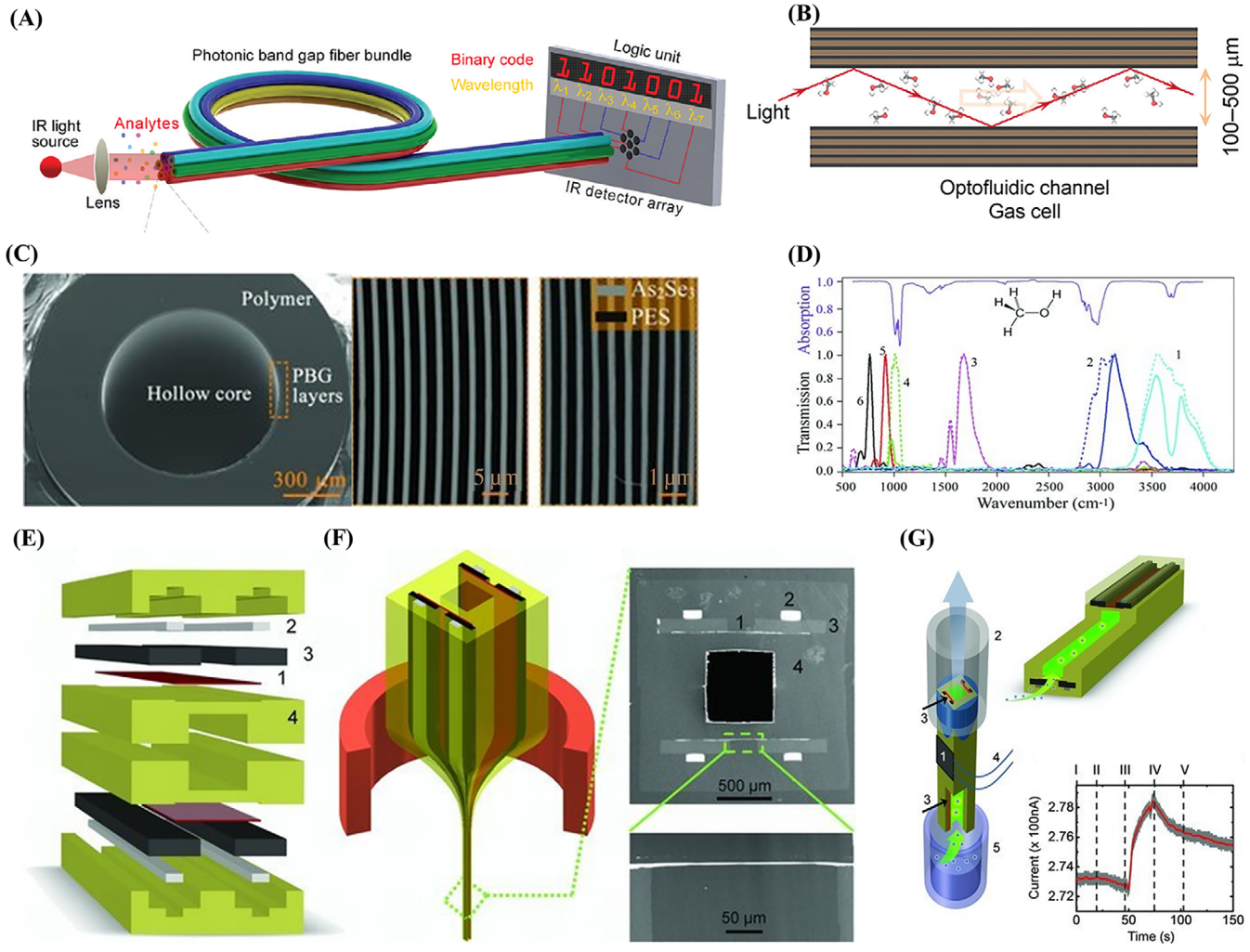

FIGURE 5 Multimaterial fibers for optoelectronic sensing. (A) Schematic drawings of the digital optoelectronic nose. Reproduced with permission.[99] Copyright 2012, American Chemical Society. (B) Enhanced electromagnetic interaction between the guided light and analytes present in the core of fibers. Reproduced with permission.[99] Copyright 2012, American Chemical Society. (C) SEM images of the cross-section of photonic bandgap fiber and enlarged images of the photonic bandgap structures with different periods. Reproduced with permission.[100] Copyright 2011, John Wiley and Sons. (D) Fiber array transmission and its quenching upon methanol introduction, before (dashed) and after (solid). Reproduced with permission.[100] Copyright 2011, John Wiley and Sons. (E) Schematic of the preform assembly. Reproduced with permission.[101] Copyright 2012, John Wiley and Sons. (F) Schematics of the thermal drawing process and the SEM images showing the structural cross-section of the fabricated fiber. Reproduced with permission.[101] Copyright 2012, John Wiley and Sons. (G) Schematic of the optoelectronic chemical measurement scheme and a typical chemical luminescence excited photocurrent measured by the device. Reproduced with permission.[101] Copyright 2012, John Wiley and Sons

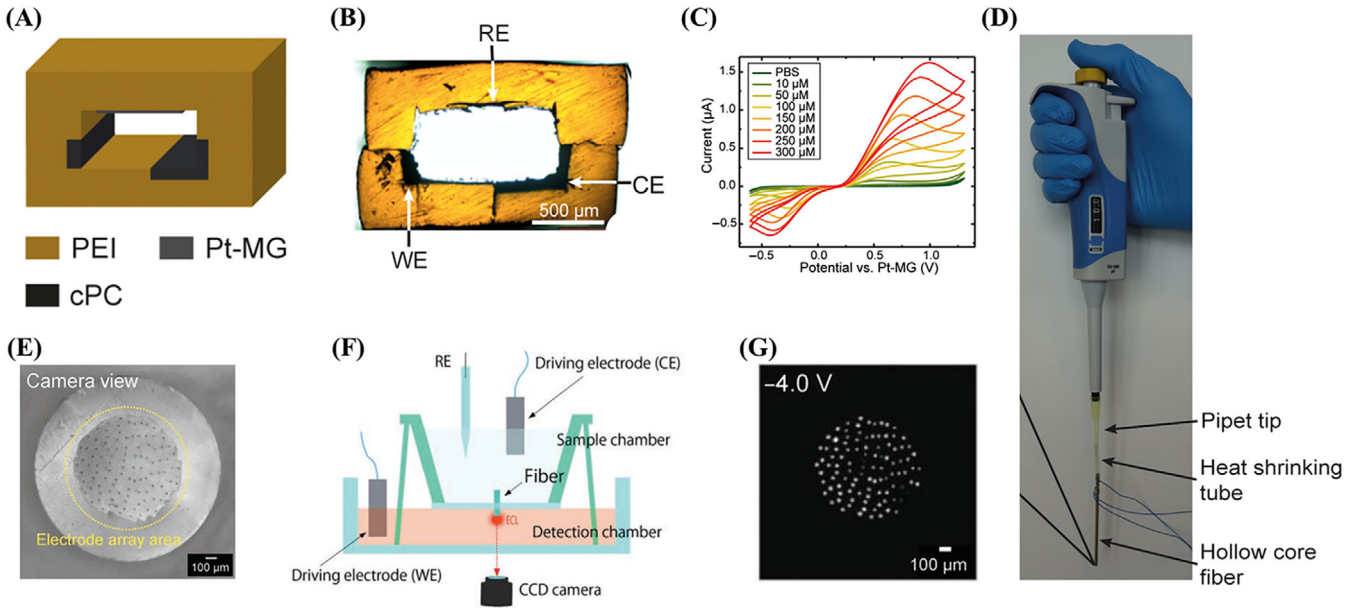

FIGURE 6 Electrochemical sensing. (A,B) Schematic and optical micrograph of the hollow core fiber cross-section, respectively. Reproduced with permission.[98] Copyright 2021, American Chemical Society. (C) Cyclic voltammograms for paracetamol concentrations between 10 and 300 μM. Reproduced with permission.[98] Copyright 2021, American Chemical Society. (D) Schematic of the hollow core electrochemical fiber attached to a pipet tip via heat-shrink tubing. Reproduced with permission.[98] Copyright 2021, American Chemical Society. (E) An optical micrograph of the multi-electrode fiber. Reproduced with permission.[97] Copyright 2021, John Wiley and Sons. (F) Schematic of the measurement system. Reproduced with permission.[97] Copyright 2021, John Wiley and Sons. (G) Images of the surface of the multi-electrode fiber obtained using the CCD camera during the potential sweep. Reproduced with permission.[97] Copyright 2021, John Wiley and Sons

and interact with their surroundings. Owing to the flexibility of the thermal drawing technique in designing the fiber structures and functional materials, numerous thermally drawn tactile sensing fibers have been developed for smart textiles and wearable devices. Nguyen-Dang et al. firstly reported a cantilever-like fiber structure for touch sensing, as shown in Figure 7A.[102] This cantilever-like structure comprises two parts of CPC serving as two electrodes. The two CPC parts will contact each other and form a conductive path when pressed. Thus, the pressed position can be decided according to the measured resistance. As shown in Figure 7B, the measured pressure position matches well with the actual position. Due to the high resistance of the CPC, even a small change in pressure position can result in a significant change in resistance, ensuring high positioning accuracy. Apart from the pressure positioning, Qu et al. introduced a thermoplastic elastomer, styrene–ethylene–butylene–styrene (SEBS), as the supporting material and achieved several tactile sensing purposes.[103] Benefiting from the high flexibility and stretchability of the elastomer, the as-drawn SEBS fiber could be stretched to more than 500% of its original length. By incorporating several CPE electrodes into the SEBS fiber, both the position and pressure direction of the touched point could be detected, as shown in Figure 7C,D.

Moreover, by altering the fiber structure and using highly malleable liquid metal electrodes, force magnitude and fiber strain can be detected by measuring resistance and capacity change (Figure 7E,F). In addition to these tactile sensing fibers based on resistance or capacity change, Figure 7G demonstrates a fully distributed tactile sensing fiber integrating two parallel copper (Cu) wires.[15] Its sensing principle is based on the impedance change caused by the distance between two Cu wires or materials' permittivity. In this work, frequency domain reflectometry is used to measure the impedance variation along with the fiber. The interrogation signal will be partially reflected at each pushed place since the distance between two Cu wires changes when pressed. As a result, each pressed position could be figured out by measuring the time delay for each reflected signal, leading to multipoint distributed tactile sensing (Figure 7H).

Additionally, localized temperature changes along the fiber could also be detected due to thermal expansion and the changed permittivity. Similarly, Sorin et al. proposed a stretchable transmission line for distributed mechanical sensing through electrical reflectometry.[104] This thermally drawn transmission line includes elastomer dielectric and liquid metal electrodes. Multimodal deformations, such as strain sensing, pressure sensing,

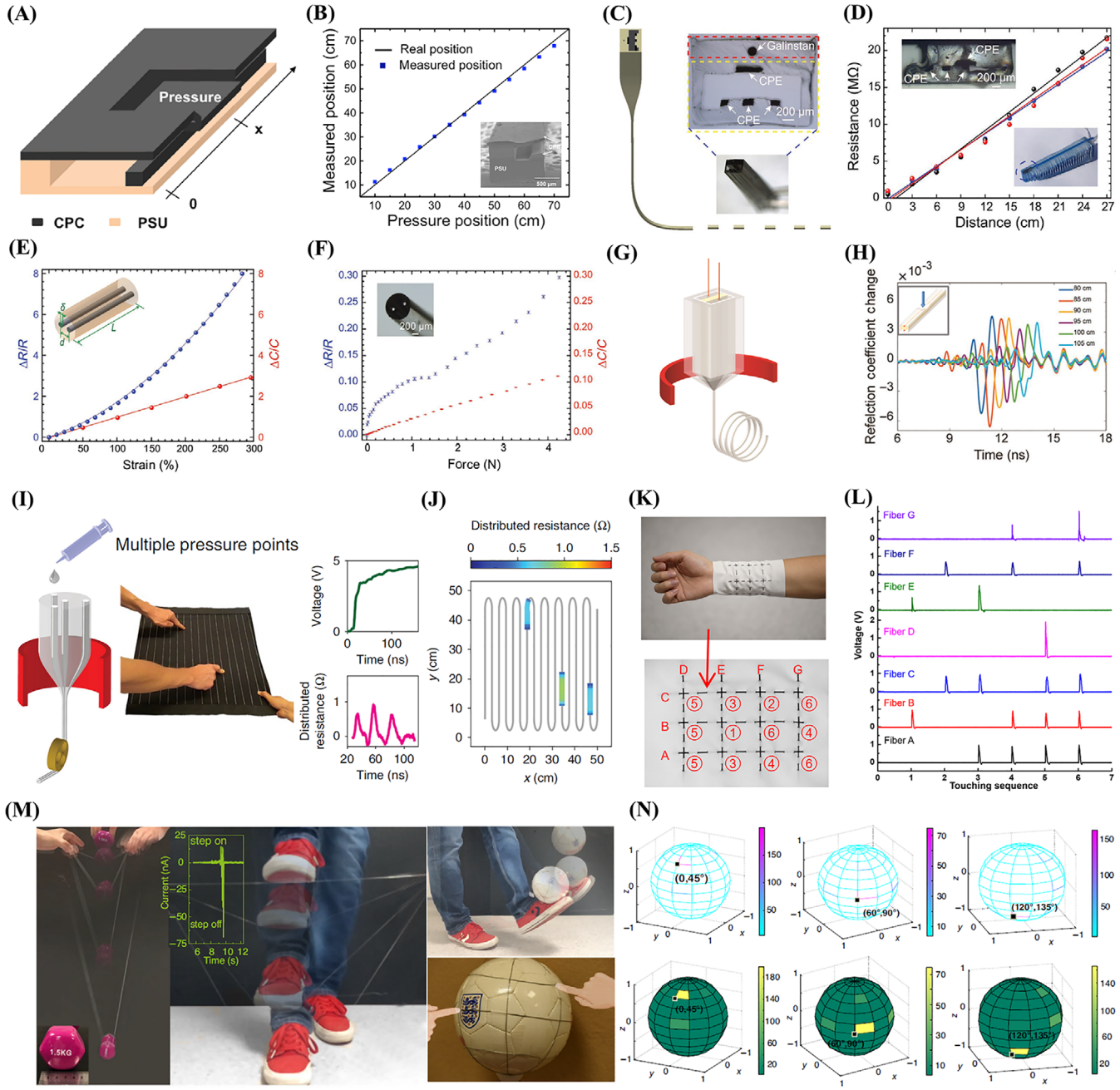

FIGURE 7 Thermally drawn fibers for tactile sensing. (A,B) Cantilever-like fiber structure for pressure positioning. Reproduced with permission.[102] Copyright 2017, IOP Publishing. (C,D) SEBS/CPE fiber for pressure position and force direction sensing. Reproduced with permission.[103] Copyright 2018, John Wiley and Sons. (E,F) SEBS/liquid metal fiber for strain and pressure sensing. Reproduced with permission.[103] Copyright 2018, John Wiley and Sons. (G) Fully distributed tactile sensing fiber integrating two parallel copper wires. Reproduced with permission.[15] Copyright 2020, John Wiley and Sons. (H) Measured interrogation signal when pressing different positions. Reproduced with permission.[15] Copyright 2020, John Wiley and Sons. (I) Thermally drawn stretchable transmission line for distributed mechanical sensing. Reproduced with permission.[104] Copyright 2020, Springer Nature. (J) Distributed resistance profile. Reproduced with permission.[104] Copyright 2020, Springer Nature. (K,L) Self-powered multi-point touch sensing fabric. Reproduced with permission.[51] Copyright 2020, Springer Nature. (M) Superelastic and conductive SEBS fiber that can withstand the impact of a free-falling dumbbell and can continue to function normally when stepped on. Reproduced with permission.[5] Copyright 2021, Springer Nature. (N) Visualized and reconstructed spherical coordinate touch sensing net. Reproduced with permission.[5] Copyright 2021, Springer Nature

and pressure positioning, could be detected from the measured distributed resistance profile by modifying the cross-sectional configuration of the fiber. As a result, the force resolution reaches 0.2 N, and the spatial resolution is <6 cm, while the strain resolution achieves 0.25%. In addition, a stretchable fabric based on the transmission line is fabricated (Figure 7I). Multiple pressure positions and pressure magnitudes could simultaneously be monitored and visualized through a MATLAB program (Figure 7J).

Self-powered tactile sensing fibers were also achieved by combining with triboelectric nano-generator (TENG) technology. Wang et al. developed a direct imprinting thermal drawing technology during the thermal drawing process to fabricate fibers with surface patterns.[51] The surface structure on the entire fiber surface could effectively enhance the TENG performance. Thus, when fiber-based TENG is touched, it can generate a voltage pulse. The surface patterned TENG fibers are then woven into a commercial fabric to create a multi-point touch sensing fabric. Figure 7K shows that the fibers are 12 nodes. A voltage pulse will be generated from the corresponding fibers when the node is pressed. Furthermore, the collected voltage signal could be used to infer the touch position (Figure 7L). In 2021, Chen et al. reported a soluble-core thermal drawing approach to further extend the material range that is compatible with the thermal drawing technique.[5] A superelastic and conductive SEBS fiber that can be stretched up to 1900% strain was fabricated. As shown in Figure 7M, this fiber can withstand the impact of a 1.5 kg free-falling dumbbell and functions normally when stepped on by a shoe. Similarly, a self-powered spherical coordinate touch sensing net is built based on superelastic and conductive SEBS fibers (Figure 7N). Furthermore, the detected signal can be used to visualize the touched point in real-time.

7 | OTHER INFORMATION FIBERS

7.1 | Biological probes

Optogenetics can stimulate and inhibit the activity of optically sensitive neurons by manipulating light, providing insight into the study of neural signals, and having promising applications in the treatment of neurological diseases.[105–107] Therefore, it is of great research value to develop a neural probe with low transmission loss, low impedance, high signal-to-noise ratio (SNR), high biocompatibility, multi-point, and long-term stable measurement.[105]

Figure 8A illustrates an all-polymer neural probe consisting of PC, conductive polyethylene (CPE), and cyclic olefin copolymer (COC) fabricated by the thermal drawing process.[108] The neural probe can maintain the functions of drug delivery, neural signal recording, and optogenetic stimulation in 2-month experiments of freely moving mice by integrating a surrounding waveguide, one microfluidic channel, and four electrodes, as shown in Figure 8B,C. The designed neural probe demonstrates a lower optical loss of 1.6 dB cm^{-1} than the reported polymer probes, whose impedance is 3–5 MΩ, equivalent to CPE at 1 kHz.[108] Park et al. developed a composite electrode with higher conductivity, consisting of CPE and graphite, to achieve a neural probe with improved optical and electrical properties, as shown in Figure 8D.[109] Based on this composite electrode, after soaking the neural probe in a phosphate-buffered saline solution, it exhibited an impedance of 0.62 ± 0.23 MΩ at 1 kHz and a lower transmission loss of 1.5 dB cm^{-1}.[109] Figure 8E shows that the multifunctional integrated and flexible neural fiber reduced brain tissue damage and improved biocompatibility during long-term signal recording.[109] Furthermore, when compared to the CPE electrode, the multi-electrode fiber probe based on tin wire with five micros diameter demonstrated excellent SNR in neural recording as illustrated in Figure 8F.[108] This multi-electrode fiber probe was prepared using a two-step thermal drawing process to obtain a tin electrode array with more wires and smaller electrode diameter.[108] The impedance of the multi-electrode fiber probe reached 892 ± 313 kΩ at 1 kHz after experimental measurement. The SNR during optical stimulation in mice was 13 ± 6.[108] Nevertheless, the selection of cladding material is determined by its glass transition temperature, which should be equivalent to the melting temperature of tin electrodes. Due to the strong absorption of light waves in the visible spectrum, the application of poly(ether imide) (PEI) in optogenetics is inevitably limited.[113] As shown in Figure 8G,H, Du et al. and Antonini et al. directly fed copper and tungsten electrode wires into the hollow polymethyl methacrylate (PMMA) to fabricate neural probes, respectively.[65,105] These metal electrode wires, with micron diameter and much higher melting temperature than PMMA's glass transition temperature, overcome the limitation of material thermal property.[65,105] The copper and the tungsten electrode exhibited the transmission loss coefficient of 1.18 ± 0.04 and 1.69 ± 0.04 dB cm^{-1}, and the SNR value of 30 and 15.6 ± 5.2, respectively.[65,105] Furthermore, Fu et al. reported a biodegradable neural probe-based poly(L-lactic acid) (PLLA), which presented a natural solution in vivo experiment, as illustrated in Figure 8I.[110] However, due to the lack of outer layer materials, the probe leaked light waves when the probe was implanted into the tissue. Some advanced neural probes have been developed to promote the

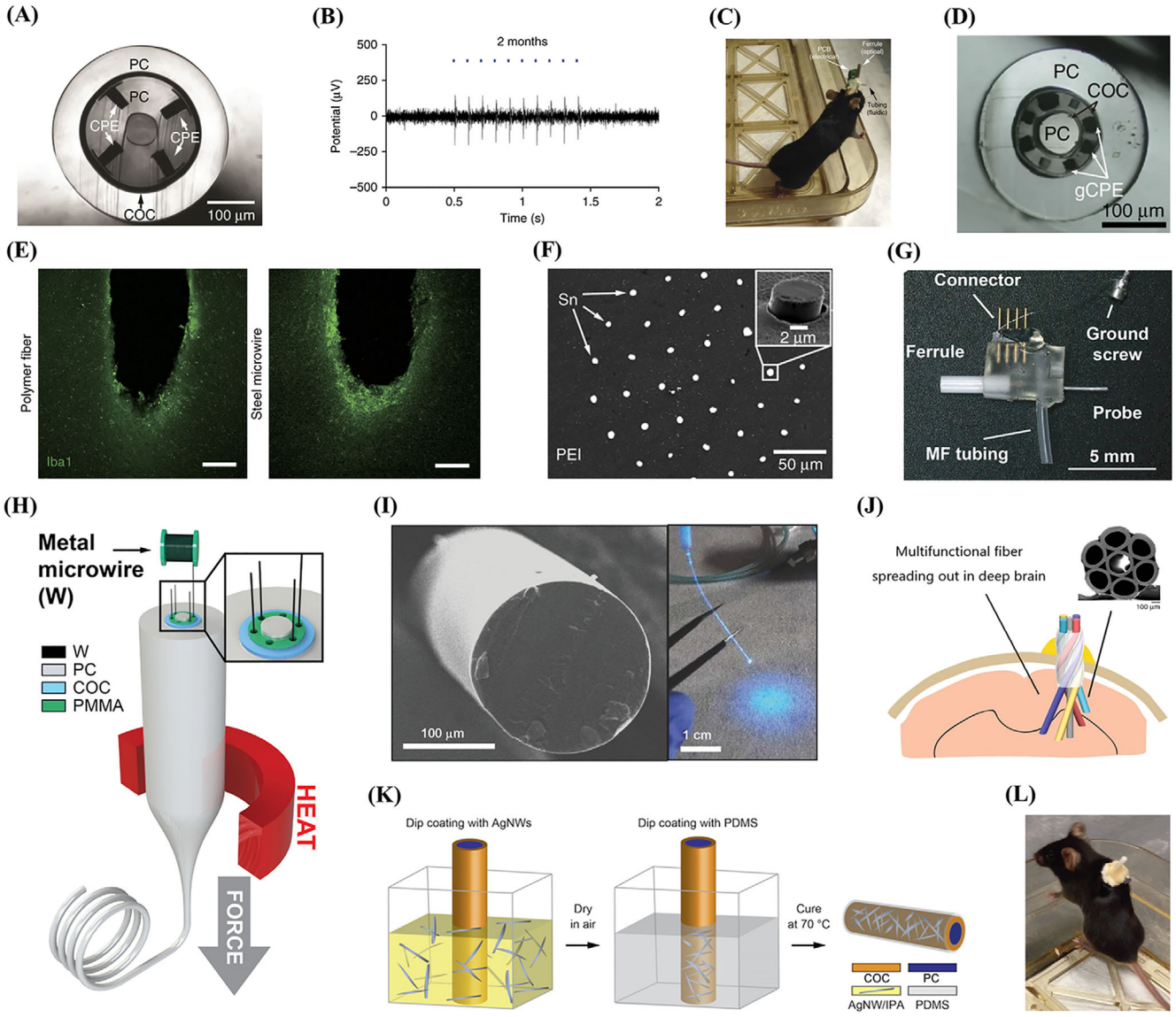

FIGURE 8 (A) Cross-sectional image of the all-polymer neural probe. Reproduced with permission.[108] Copyright 2015, Springer Nature. (B) Image of the electrical signal generated by photo-genetic stimulation. Reproduced with permission.[108] Copyright 2015, Springer Nature. (C) Photograph of the mouse in neural exploration experiment. Reproduced with permission.[108] Copyright 2015, Springer Nature. (D) Cross-sectional image of the neural probe with composite electrodes (conductive polyethylene (CPE) and graphite). Reproduced with permission.[109] Copyright 2017, Springer Nature. (E) Images of peripheral glial scar and blood–brain barrier destruction after polymer fiber and metal nanowire implantation. Reproduced with permission.[109] Copyright 2017, Springer Nature. (F) Cross-sectional image of the multi-electrode fiber. Reproduced with permission.[108] Copyright 2015, Springer Nature. (G) Photograph of the device integrating neural probes. Reproduced with permission.[65] Copyright 2021, Wiley-VCH. (H) Schematic diagram of the thermal drawing process (containing metal nanowires). Reproduced with permission.[65] Copyright 2021, Wiley-VCH. (I) Cross-sectional image of the PLLA fiber and photograph of the bent PLLA fiber coupled to a blue LED. Reproduced with permission.[110] Copyright 2017, WILEY-VCH. (J) Multiple fibers are inserted deep into the brain. The insert shows a cross-sectional image of the scaffolding fiber containing seven hollow channels. Reproduced with permission.[111] Copyright 2020, Springer Nature. (K) Schematic diagram of preparing flexible neural probes. Reproduced with permission.[112] Copyright 2017, AAAS. (L) Image of mouse implanted with a spinal probe. Reproduced with permission.[112] Copyright 2017, AAAS

development of optogenetics and understanding of the nervous system. For example, Jiang et al. prepared a multisite neural probe that provides 3D records of brain tissue when introduced into the brain at different specific angles by designing hollow helix channels, as shown in Figure 8J.[111] Lu et al. reported a bendable and stretchable

spinal probe to meet repeated deformation of the spine during normal movement. The preform composed of PC and COC was drawn into a flexible fiber, and then Ag nanowires and polydimethylsiloxane (PDMS) were directly coated on the fiber surface in sequence, as illustrated in Figure 8K,L.[112] Compared with the existing research, the combination of functional fibers and soft hydrogel matrix prolongs the stable monitoring term due to the reduction of biomechanical mismatch with the neural tissue.[114] Furthermore, thermally drawn fibers exhibit distinctive advantages in in-line biochemical sensing, as shown in Figure 9A. They have achieved a wide range of analytes, including methylene blue absorptive molecules, nonspecific liquid refractive index detection, and human cardiac troponin T molecules.[115]

7.2 | Energy fibers

Energy fibers have become candidates for flexible electric generators and energy-storage systems to continuously supply power for wearable electronic devices.[119] The existing material systems with good performance, such as thermoelectric materials, triboelectric materials, and supercapacitors, are respectively synthesized into energy fibers by thermal drawing, which ensures the efficiency of energy supply and has the potential of weaving into fabrics. Thermoelectric fiber can generate electric energy by using the temperature difference between the human body and the environment. Based on the principle of the Seebeck effect. Zhang et al. prepared p-type and n-type fibers composed of $Bi_{0.5}Sb_{1.5}Te_3$ and Bi_2Se_3 and measured the thermoelectric merit (ZT), as illustrated in Figure 9D.[117] The p-type and n-type fibers demonstrated ZTs of 1.25 and 0.23 at 300 K, respectively, and generated maximum output power of 0.36 W at a temperature difference of 50 K, as shown in Figure 9E.[117] Besides that, research on thermally drawn thermoelectric fiber has focused on In_4Se_3 core thermoelectric fiber,[49] polycrystalline SnSe core thermoelectric fiber,[50] and single-crystal SnSe thermoelectric fiber.[53] Significantly, the single-crystal SnSe thermoelectric fiber has the highest ZT value of 1.94 and can generate the output voltage of 30 mV at the temperature difference of 10 K.[53]

In addition to utilizing thermal energy to generate electricity from the human body sustainably, TENGs can also power electric devices using contact electrification and electrostatic induction effects.[33] As shown in Figure 9F, Dong et al. introduced a high-output triboelectric fiber, which integrated the surface microstructure with four liquid metal electrodes.[33] When external materials (e.g., PMMA) get into contact and separate from the fiber surface, the charges around the metal electrodes are moved, resulting in the change of electric field.[33] After integrating triboelectric fibers into 2D textiles, the open-circuit voltage V_{oc} and short-circuit transferred charge Q_{sc} triggered by hand tapping reached 490 V and 175 nC, respectively.[33] Furthermore, triboelectric fibers were manufactured using a direct drawing metal electrode wire method, which produced open-circuit voltage V_{oc} and short-circuit transferred charge Q_{sc} of 27.8 V and 14.1 nC when applied with a force of 70 N at a frequency of 8 Hz.[120]

7.3 | Integrated circuit fibers

Although thermally drawn fiber-based devices have demonstrated many functions, their performance, and functional categories are generally inferior to those of wafer processed, such as light-emitting diodes, chips, electronics for optical detected magnetic resonance (ODMR), and so on.[63,116,118] Rein et al. demonstrated the technique of combining thermal drawing process with prefabricated semiconductor devices, which realized circuit connection and devices packaging at the same time, as illustrated in Figure 9C.[116] During the thermal drawing process, the distance between the two electrodes gradually decreased in the necking region of the preform and then made contact with the electronic components located in the center.[116] The light-emitting and photodetection fibers were prepared and integrated into fabrics to achieve the function of fabric-to-fabric communication, as shown in Figure 9B,H.[116] Loke et al. demonstrated a digital fiber coupled to thermal sensing, data storage, program operation, and information processing, as shown in Figure 9G.[63] Furthermore, Figure 9I illustrates a distributed magnetic field sensor made of silica fiber for ODMR. It performs the function of detecting the position and intensity of the magnetic fields with a length of 100 m.[118]

8 | CONCLUSION AND OUTLOOK

The multifunctional fibers that rely on the state-of-the-art preform-to-fiber fabrication technique have achieved vigorous development in recent years and injected new vitality into the communication technology. Thermally drawn multimaterial fibers with multifarious functions beyond the fundamental optical information transmission have been successfully demonstrated. For example, the multifunctional fibers can mimic the five senses of the human body and work as the information acquisition device. By incorporating photoelectric semiconductor material, piezoelectric material, thermoelectric material, capacitors, or reactive chemicals into the fiber through

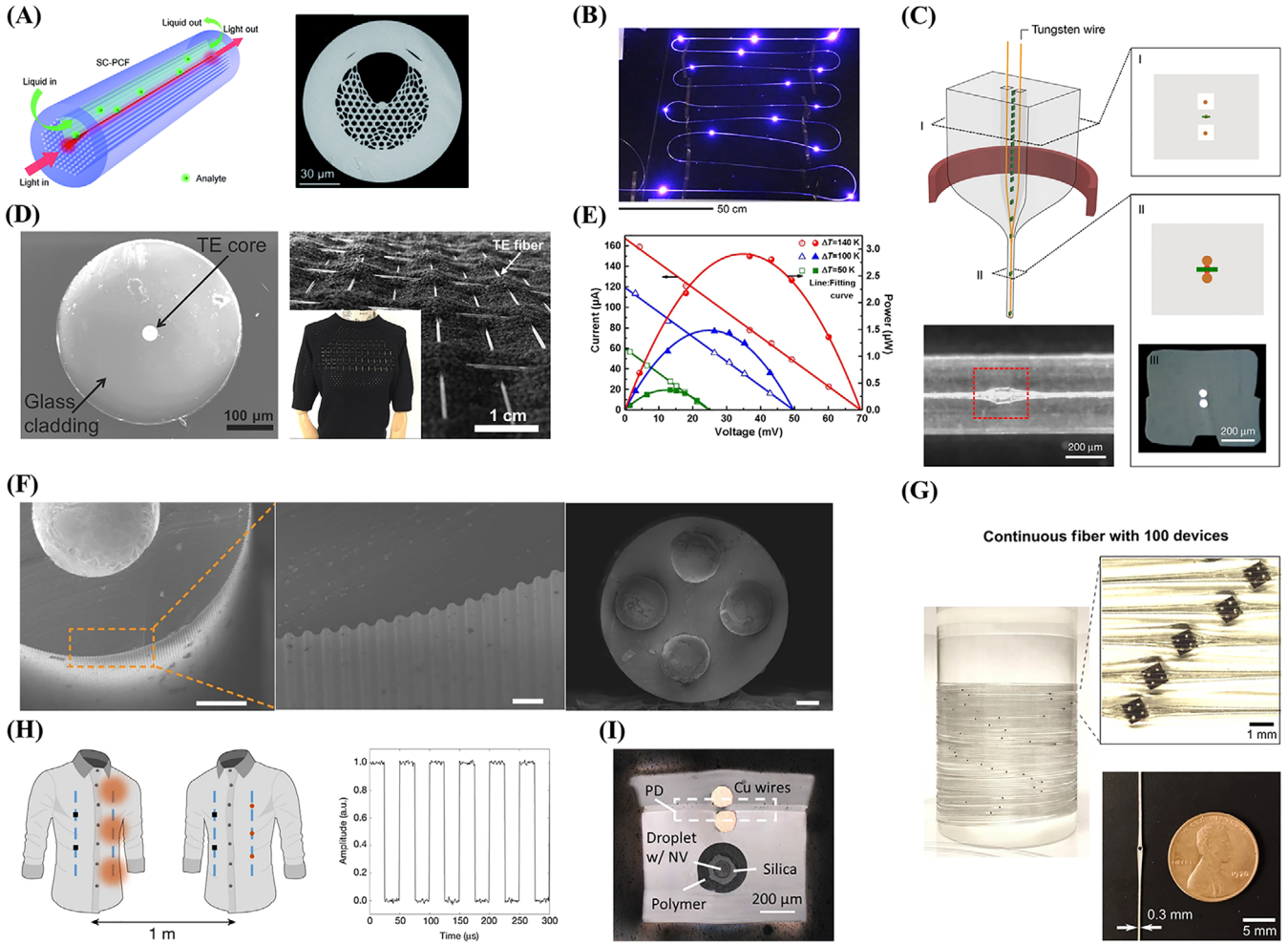

FIGURE 9 (A) Schematic diagram and SEM image of the analyte detection fiber. Reproduced with permission.[115] Copyright 2018, Royal Society of Chemistry. (B) Image of the light-emitting fibers. Reproduced with permission.[116] Copyright 2018, Springer Nature. (C) Schematic diagram of the preform drawing process. Front and cross-sectional photographs of the fiber. Reproduced with permission.[116] Copyright 2018, Springer Nature. (D) Cross-sectional SEM image of the thermoelectric fiber and photograph of the wearable thermoelectric device woven by thermoelectric fibers. Reproduced with permission.[117] Copyright 2017, Elsevier. (E) Function image of voltage, current, and output power generated by thermoelectric fibers in different temperature ranges. Reproduced with permission.[117] Copyright 2017, Elsevier. (F) Cross-sectional images of triboelectric fiber with microstructure surface and four liquid metal electrodes. Reproduced with permission.[33] Copyright 2020, Springer Nature. (G) Image of a continuous digital fiber embedded in 100 microdevices and magnified photograph of the fiber. Reproduced with permission.[63] Copyright 2021, Springer Nature. (H) Schematic diagram of the fabric-to-fabric communication system concept and the information recorded by optical detection fibers on clothes. Reproduced with permission.[116] Copyright 2018, Springer Nature. (I) Cross-sectional image of the distributed magnetic field sensor containing the electronics for optical detected magnetic resonance (ODMR) and copper wires. Reproduced with permission.[118] Copyright 2019, WILEY-VCH

the thermal drawing technique, fibers that can see images, hear the sound, feel the touch, and distinguish chemicals have come into reality. Moreover, by integrating multiple functions inside one fiber, sophisticated functions including diseases diagnosis, neural activity manipulation, in-fiber computing, inter-fiber communication, as well as energy harvest and storage have been realized, which would advance the development of human-computer interaction technology and the internet of things technology. In all, these advanced function fibers have greatly expanded and enriched the existing information technology. We can envision that new communication technologies that evolve from these advanced functional fibers and fabrics may infiltrate into every corner of our daily lives in the near future. Here, we summarize some remaining challenges and possible future directions for the thermally drawn multifunctional fibers.

1. The material library for thermal drawing is still insufficient. Generally, the core materials and the cladding materials are desired to have a similar melting temperature or glass transition temperature so that the macroscopic preform made of these different materials can shrink into fibers when being heated at a higher temperature. This prerequisite further limits the number of available glasses, thermal plastics, and metals that can be co-drawn. In this respect, material scientists may relieve the restriction by developing new materials with diverse thermal properties and adjusting the thermal properties of existing materials through chemical modifications. On the other hand, innovative thermal drawing strategies may expand the available material database. One breakthrough is the convergence fiber drawing approach, which allows high-temperature metal electrodes and silica optical fibers to be co-drawn with low-temperature polymer simultaneously into a single complexed fiber. More innovations are expected further to expand the available functional materials for thermal drawing. For example, the in-line UV/heat curing epoxy coating procedure, which is traditionally employed to provide mechanical protection for silica optical fibers, may be adopted to add functional coatings to the as-drawn multifunctional fibers.
2. An unavoidable issue is that the performance of these in-fiber optoelectronic devices, thermoelectric devices, piezoelectric devices, and electronic devices are generally inferior to those prepared by the standard silicon wafer processing. This is because the functional semiconductor core materials are common in an amorphous or polycrystalline state, which significantly degrades their performance. To tackle this problem, researchers have developed postprocessing techniques like thermal annealing and laser recrystallization to convert the amorphous/polycrystalline fiber core to a single crystalline state, improving the device's performance. In future studies, various solutions may be presented. On the one hand, high-performance semiconductor materials that can retain their properties during the thermal drawing process are expected. On the other hand, versatile postprocessing techniques will be developed by researchers to enhance the functionality of the in-fiber devices to a degree comparable to chip-based devices.
3. Although the multifunctional fiber has demonstrated multifunctions such as photodetection, imaging, acoustoelectric detection, chemical sensing, tactile sensing, biological probing, energy harvesting and storage, data storage, program operation, as well as information processing, these demonstrated applications studies are relatively simple, and many efforts are needed to perfect the in-fiber devices, as well as the relevant systems. In addition, the functions mentioned above have been demonstrated individually with a specific fiber design. Multifunction fusion in a single fiber has seldomly been explored. The challenge lies in that the functional materials to deliver different functions should have identical thermal properties, and moreover, crosstalk between different functions should be effectively suppressed. Much more effort will be put into multifunction integration in future studies.

ACKNOWLEDGMENTS

Yanan Shen, Zhe Wang, Zhixun Wang, and Jiajia Wang contributed equally to this work. This work was supported by the National Natural Science Foundation of China (52172249, 62005101, and 51976215), the Scientific Instrument Developing Project of the Chinese Academy of Sciences (YJKYYQ20200017), and the Funding of Innovation Academy for Light-duty Gas Turbine, Chinese Academy of Sciences (CXYJJ21-ZD-02). This work was supported by the Singapore Ministry of Education Academic Research Fund Tier 2 (MOE2019-T2-2-127 and MOE-T2EP50120-0002), A*STAR under AME IRG (A2083c0062), the Singapore Ministry of Education Academic Research Fund Tier 1 (MOE2019-T1-001-103 (RG 73/19) and MOE2019-T1-001-111 (RG90/19)), and the Singapore National Research Foundation Competitive Research Program (NRF-CRP18-2017-02). This work was partly supported by the Schaeffler Hub for Advanced Research at NTU, under the ASTAR IAF-ICP Programme ICP1900093. This work was also supported by Nanyang Technological University.

CONFLICT OF INTEREST

The authors declare no conflict of interest.

ORCID

Haisheng Chen https://orcid.org/0000-0002-1383-9476
Kaiwei Li https://orcid.org/0000-0001-5022-1897
Lei Wei https://orcid.org/0000-0003-0819-8325
Ting Zhang https://orcid.org/0000-0001-5967-0525

REFERENCES

1. Tao G, Abouraddy AF, Stolyarov AM. Multimaterial fibers. *Int J Appl Glass Sci*. 2012;3(4):349-368.
2. Loke G, Yan W, Khudiyev T, Noel G, Fink Y. Recent progress and perspectives of thermally drawn multimaterial fiber electronics. *Adv Mater*. 2020;32(1):1904911.
3. Abouraddy AF, Bayindir M, Benoit G, et al. Towards multimaterial multifunctional fibres that see, hear, sense and communicate. *Nat Mater*. 2007;6(5):336-347.

4. Schmidt MA, Argyros A, Sorin F. Hybrid optical fibers—an innovative platform for in-fiber photonic devices. *Adv Opt Mater*. 2016;4(1):13-36.
5. Chen M, Wang Z, Zhang Q, et al. Self-powered multifunctional sensing based on super-elastic fibers by soluble-core thermal drawing. *Nat Commun*. 2021;12(1):1416.
6. Sorin F, Shapira O, Abouraddy AF, et al. Exploiting collective effects of multiple optoelectronic devices integrated in a single fiber. *Nano Lett*. 2009;9(7):2630-2635.
7. Russell P. Photonic crystal fibers. *Science*. 2003;299(5605): 358-362.
8. Graham-Rowe D. Fibres get functional. *Nat Photon*. 2011;5(2): 66-67.
9. Russell PSJ. Photonic-crystal fibers. *Journal of Lightwave Technology*. 2006;24(12):4729-4749.
10. Pan Z, Yang J, Li L, et al. All-in-one stretchable coaxial-fiber strain sensor integrated with high-performing supercapacitor. *Energy Storage Materials*. 2020;25:124-130.
11. Yan W, Dong C, Xiang Y, et al. Thermally drawn advanced functional fibers: new frontier of flexible electronics. *Mater Today*. 2020;35:168-194.
12. Leber A, Cholst B, Sandt J, Vogel N, Kolle M. Stretchable thermoplastic elastomer optical fibers for sensing of extreme deformations. *Adv Funct Mater*. 2019;29(5):1802629.
13. Zhang Y, Li X, Kim J, et al. Thermally drawn stretchable electrical and optical fiber sensors for multimodal extreme deformation sensing. *Adv Opt Mater*. 2021;9(6):2001815.
14. Lee Y, Canales A, Loke G, Kanik M, Fink Y, Anikeeva P. Selectively micro-patternable fibers via in-fiber photolithography. *ACS Cent Sci*. 2020;6(12):2319-2325.
15. Yu L, Parker S, Xuan H, et al. Flexible multi-material fibers for distributed pressure and temperature sensing. *Adv Funct Mater*. 2020;30(9):1908915.
16. Yan W, Richard I, Kurtuldu G, et al. Structured nanoscale metallic glass fibres with extreme aspect ratios. *Nat Nanotechnol*. 2020;15(10):875-882.
17. Bayindir M, Abouraddy AF, Shapira O, et al. Kilometer-long ordered nanophotonic devices by preform-to-fiber fabrication. *IEEE J Sel Top Quantum Electron*. 2006;12(6):1202-1213.
18. Koppes RA, Park S, Hood T, et al. Thermally drawn fibers as nerve guidance scaffolds. *Biomaterials*. 2016;81:27-35.
19. Zhang T, Wang Z, Srinivasan B, et al. Ultraflexible glassy semiconductor fibers for thermal sensing and positioning. *ACS Appl Mater Interfaces*. 2019;11(2):2441-2447.
20. Cheng Y, Wang R, Sun J, Gao L. A stretchable and highly sensitive graphene-based fiber for sensing tensile strain, bending, and torsion. *Adv Mater*. 2015;27(45):7365-7371.
21. Wei Y, Chen S, Yuan X, Wang P, Liu L. Multiscale wrinkled microstructures for piezoresistive fibers. *Adv Funct Mater*. 2016;26(28):5078-5085.
22. Shim BS, Chen W, Doty C, Xu C, Kotov NA. Smart electronic yarns and wearable fabrics for human biomonitoring made by carbon nanotube coating with polyelectrolytes. *Nano Lett*. 2008;8(12):4151-4157.
23. Yang A, Li Y, Yang C, et al. Fabric organic electrochemical transistors for biosensors. *Adv Mater*. 2018;30(23):1800051.
24. Park J, Jin K, Sahasrabudhe A, et al. In situ electrochemical generation of nitric oxide for neuronal modulation. *Nat Nanotechnol*. 2020;15(8):690-697.
25. Park J, Zeng JS, Sahasrabudhe A, et al. Electrochemical modulation of carbon monoxide-mediated cell signaling. *Angew Chem Int Ed*. 2021;60(37):20325-20330.
26. Wang L, Wang L, Zhang Y, et al. Weaving sensing fibers into electrochemical fabric for real-time health monitoring. *Adv Funct Mater*. 2018;28(42):1804456.
27. Jost K, Dion G, Gogotsi Y. Textile energy storage in perspective. *J Mater Chem A*. 2014;2(28):10776-10787.
28. Li P, Jin Z, Peng L, et al. Stretchable all-gel-state fiber-shaped supercapacitors enabled by macromolecularly interconnected 3D graphene/nanostructured conductive polymer hydrogels. *Adv Mater*. 2018;30(18):1800124.
29. Zhang Q, Li C, Li Q, et al. Flexible and high-voltage coaxial-fiber aqueous rechargeable zinc-ion battery. *Nano Lett*. 2019; 19(6):4035-4042.
30. Yang Z, Deng J, Sun X, Li H, Peng H. Stretchable, wearable dye-sensitized solar cells. *Adv Mater*. 2014;26(17):2643-2647.
31. Li H, Guo J, Sun H, Fang X, Wang D, Peng H. Stable hydrophobic ionic liquid gel electrolyte for stretchable fiber-shaped dye-sensitized solar cell. *Chem*. 2015;1(6):399-402.
32. He X, Zi Y, Guo H, et al. A highly stretchable fiber-based triboelectric nanogenerator for self-powered wearable electronics. *Adv Funct Mater*. 2017;27(4):1604378.
33. Dong C, Leber A, Das Gupta T, et al. High-efficiency super-elastic liquid metal based triboelectric fibers and textiles. *Nat Commun*. 2020;11(1):3537.
34. Shabahang S, Clouser F, Shabahang F, Yun S-H. Single-mode, 700%-stretchable, elastic optical fibers made of thermoplastic elastomers. *Adv Opt Mater*. 2021;9(12):2100270.
35. Yan W, Qu Y, Das Gupta T, et al. Semiconducting nanowire-based optoelectronic fibers. *Adv Mater*. 2017;29(27):1700681.
36. Zhang J, Wang Z, Wang Z, Wei L. Advanced multi-material optoelectronic fibers: a review. *J Light Technol*. 2021;39(12): 3836-3845.
37. Shi J, Liu S, Zhang L, et al. Smart textile-integrated microelectronic systems for wearable applications. *Adv Mater*. 2020; 32(5):1901958.
38. Zhang YJ, Zhang Q, Li YB, Wang NL, Zhu J. Coating of carbon nanotubes with tungsten by physical vapor deposition. *Solid State Commun*. 2000;115(1):51-55.
39. Li C, Xie B, Chen J, He Z, Chen Z, Long Y. Emerging mineral-coupled composite phase change materials for thermal energy storage. *Energ Conver Manage*. 2019;183:633-644.
40. Li Y, Huang Z, Huang K, Carnahan D, Xing Y. Hybrid Li-air battery cathodes with sparse carbon nanotube arrays directly grown on carbon fiber papers. *Energ Environ Sci*. 2013;6(11): 3339-3345.
41. Liang DX, Yang HR, Finefrock SW, Wu Y. Flexible nanocrystal-coated glass fibers for high-performance thermoelectric energy harvesting. *Nano Lett*. 2012;12(4):2140-2145.
42. Li X, Hua T, Xu B. Electromechanical properties of a yarn strain sensor with graphene-sheath/polyurethane-core. *Carbon*. 2017;118:686-698.
43. Frutiger A, Muth JT, Vogt DM, et al. Capacitive soft strain sensors via multicore-shell fiber printing. *Adv Mater*. 2015; 27(15):2440-2446.
44. Kim SJ, We JH, Cho BJ. A wearable thermoelectric generator fabricated on a glass fabric. *Energ Environ Sci*. 2014;7(6):1959-1965.

45. Xu WH, Shi Y, Hadim H. The fabrication of thermoelectric $La_{0.95}Sr_{0.05}CoO_3$ nanofibers and Seebeck coefficient measurement. *Nanotechnol*. 2010;21(39):395303.
46. Reneker DH, Chun I. Nanometre diameter fibres of polymer, produced by electrospinning. *Nanotechnology*. 1996;7(3): 216-223.
47. Wen NX, Fan Z, Yang ST, et al. Highly conductive, ultraflexible and continuously processable PEDOT:PSS fibers with high thermoelectric properties for wearable energy harvesting. *Nano Energy*. 2020;78:105361.
48. Xu H, Guo Y, Wu B, et al. Highly integrable thermoelectric fiber. *ACS Appl Mater Interfaces*. 2020;12(29):33297-33304.
49. Sun M, Tang G, Qian G, et al. In_4Se_3 alloy core thermoelectric fibers. *Mater Lett*. 2018;217:13-15.
50. Sun M, Tang G, Liu W, et al. Sn-Se alloy core fibers. *J Alloys Compd*. 2017;725:242-247.
51. Wang Z, Wu T, Wang Z, et al. Designer patterned functional fibers via direct imprinting in thermal drawing. *Nat Commun*. 2020;11(1):3842.
52. Tung N-D, de Luca AC, Yan W, et al. Controlled submicrometer hierarchical textures engineered in polymeric fibers and microchannels via thermal drawing. *Adv Funct Mater*. 2017;27(10):1605935.
53. Zhang J, Zhang T, Zhang H, et al. Single-crystal SnSe thermoelectric fibers via laser-induced directional crystallization: from 1D fibers to multidimensional fabrics. *Adv Mater*. 2020; 32(36):2002702.
54. Loke G, Yuan R, Rein M, et al. Structured multimaterial filaments for 3D printing of optoelectronics. *Nat Commun*. 2019; 10(1):4010.
55. Gumennik A, Levy EC, Grena B, et al. Confined in-fiber solidification and structural control of silicon and silicon-germanium microparticles. *Proc Natl Acad Sci U S A*. 2017; 114(28):7240-7245.
56. Dai Y, Du M, Feng X, Zhang W, Zhou S. Microstructured multimaterial fibers for efficient optical detection. *J Am Ceram Soc*. 2021;104(8):4058-4064.
57. Yan W, Tung N-D, Cayron C, et al. Microstructure tailoring of selenium-core multimaterial optoelectronic fibers. *Opt Mater Express*. 2017;7(4):1388-1397.
58. Khudiyev T, Lee JT, Cox JR, et al. 100 m Long thermally drawn supercapacitor fibers with applications to 3D printing and textiles. *Adv Mater*. 2020;32(49):2004971.
59. Yuan R, Nagarajan MB, Lee J, Voldman J, Doyle PS, Fink Y. Designable 3D microshapes fabricated at the intersection of structured flow and optical fields. *Small*. 2018;14(50):1803585.
60. Wang S, Zhang T, Li K, et al. Flexible piezoelectric fibers for acoustic sensing and positioning. *Adv Electron Mater*. 2017; 3(3):1600449.
61. Yildirim A, Ozturk FE, Bayindir M. Smelling in chemically complex environments: an optofluidic Bragg fiber array for differentiation of methanol adulterated beverages. *Anal Chem*. 2013;85(13):6384-6391.
62. Adamu AI, Ozturk FE, Bayindir M. Binary coded identification of industrial chemical vapors with an optofluidic nose. *Appl Optics*. 2016;55(36):10247-10254.
63. Loke G, Khudiyev T, Wang B, et al. Digital electronics in fibres enable fabric-based machine-learning inference. *Nat Commun*. 2021;12(1):3317.
64. Chin AL, Jiang S, Jang E, et al. Implantable optical fibers for immunotherapeutics delivery and tumor impedance measurement. *Nat Commun*. 2021;12(1):5138.
65. Antonini M-J, Sahasrabudhe A, Tabet A, et al. Customizing MRI-compatible multifunctional neural interfaces through fiber drawing. *Adv Funct Mater*. 2021;31(43):2104857.
66. Yan W, Page A, Tung N-D, et al. Advanced multimaterial electronic and optoelectronic fibers and textiles. *Adv Mater*. 2019;31(1):1802348.
67. Gierej A, Filipkowski A, Pysz D, et al. On the characterization of novel step-index biocompatible and biodegradable poly (D, L-lactic acid) based optical fiber. *J Light Technol*. 2020;38(7): 1905-1914.
68. Maldonado A, Lemière A, Désévédavy F, et al. Elaboration of multimaterials optical fibers combining tellurite glass and metal for electro-optical applications; International Society for Optics and Photonics; 2020; 113570U.
69. Guzman F, Craig C, Moog BJ, Ravagli A, Morgan KA, Hewak DW. Manufacturing of GLS-Se glass rods and structured preforms by extrusion for optical fiber drawing for the IR region. *Opt Eng*. 2021;60(4):045101.
70. Tao G, Shabahang S, Dai S, Abouraddy AF. Multimaterial disc-to-fiber approach to efficiently produce robust infrared fibers. *Opt Mater Express*. 2014;4(10):2143-2149.
71. Ghebrebrhan M, Loke GZJ, Fink Y. Fabrication and measurement of 3D printed retroreflective fibers. *Opt Mater Express*. 2019;9(8):3432-3438.
72. Talataisong W, Ismaeel R, Marques THR, et al. Mid-IR hollow-core microstructured fiber drawn from a 3D printed PETG preform. *Sci Rep*. 2018;8(1):8113.
73. Wang Y, Wei S, Cavillon M, et al. Thermal stability of type II modifications inscribed by femtosecond laser in a fiber drawn from a 3D printed preform. *Appl Sci*. 2021;11(2):600.
74. Gierej A, Vagenende M, Filipkowski A, et al. Poly (D, L-lactic acid)(PDLLA) biodegradable and biocompatible polymer optical fiber. *J Light Technol*. 2019;37(9):1916-1923.
75. Shabahang S, Tan FA, Perlstein JD, et al. Robust multimaterial chalcogenide fibers produced by a hybrid fiber-fabrication process. *Opt Mater Express*. 2017;7(7):2336-2345.
76. Deng DS, Orf ND, Abouraddy AF, et al. In-fiber semiconductor filament arrays. *Nano Lett*. 2008;8(12):4265-4269.
77. Weng W, Yang J, Zhang Y, et al. A route toward smart system integration: from fiber design to device construction. *Adv Mater*. 2020;32(5):1902301.
78. Zhang J, Li K, Zhang T, et al. Laser-induced in-fiber fluid dynamical instabilities for precise and scalable fabrication of spherical particles. *Adv Funct Mater*. 2017;27(43):1703245.
79. Shabahang S, Kaufman JJ, Deng DS, Abouraddy AF. Observation of the Plateau-Rayleigh capillary instability in multimaterial optical fibers. *Appl Phys Lett*. 2011;99(16):161909.
80. Gumennik A, Wei L, Lestoquoy G, et al. Silicon-in-silica spheres via axial thermal gradient in-fibre capillary instabilities. *Nat Commun*. 2013;4(1):2216.
81. Rein M, Levy E, Gumennik A, Abouraddy AF, Joannopoulos J, Fink Y. Self-assembled fibre optoelectronics with discrete translational symmetry. *Nat Commun*. 2016;7(1):12807.
82. Khudiyev T, Tobail O, Bayindir M. Tailoring self-organized nanostructured morphologies in kilometer-long polymer fiber. *Sci Rep*. 2014;4(1):4864.

83. Orf ND, Shapira O, Sorin F, et al. Fiber draw synthesis. *Proc Natl Acad Sci U S A*. 2011;108(12):4743-4747.
84. Hou C, Jia X, Wei L, et al. Crystalline silicon core fibres from aluminium core preforms. *Nat Commun*. 2015;6(1):6248.
85. Bayindir M, Sorin F, Abouraddy AF, et al. Metal-insulator-semiconductor optoelectronic fibres. *Nature*. 2004;431(7010):826-829.
86. Bayindir M, Abouraddy AE, Arnold J, Joannopoulos JD, Fink Y. Thermal-sensing fiber devices by multimaterial codrawing. *Adv Mater*. 2006;18(7):845-849.
87. Sorin F, Abouraddy AF, Orf N, et al. Multimaterial photodetecting fibers: a geometric and structural study. *Adv Mater*. 2007;19(22):3872-3877.
88. Bayindir M, Shapira O, Saygin-Hinczewski D, et al. Integrated fibres for self-monitored optical transport. *Nat Mater*. 2005;4(11):820-825.
89. Abouraddy AF, Shapira O, Bayindir M, et al. Large-scale optical-field measurements with geometric fibre constructs. *Nat Mater*. 2006;5(7):532-536.
90. Sorin F, Lestoquoy G, Danto S, Joannopoulos JD, Fink Y. Resolving optical illumination distributions along an axially symmetric photodetecting fiber. *Opt Express*. 2010;18(23):24264-24275.
91. Wei L, Hou C, Levy E, et al. Optoelectronic fibers via selective amplification of in-fiber capillary instabilities. *Adv Mater*. 2017;29(1):1603033.
92. Ozgur E, Aktas O, Kanik M, Yaman M, Bayindir M. Macroscopic assembly of indefinitely long and parallel nanowires into large area photodetection circuitry. *Nano Lett*. 2012;12(5):2483-2487.
93. Egusa S, Wang Z, Chocat N, et al. Multimaterial piezoelectric fibres. *Nat Mater*. 2010;9(8):643-648.
94. Chocat N, Lestoquoy G, Wang Z, Rodgers DM, Joannopoulos JD, Fink Y. Piezoelectric fibers for conformal acoustics. *Adv Mater*. 2012;24(39):5327-5332.
95. Lu X, Qu H, Skorobogatiy M. Piezoelectric micro-and nanostructured fibers fabricated from thermoplastic nanocomposites using a fiber drawing technique: comparative study and potential applications. *ACS Nano*. 2017;11(2):2103-2114.
96. Stolyarov AM, Gumennik A, McDaniel W, et al. Enhanced chemiluminescent detection scheme for trace vapor sensing in pneumatically-tuned hollow core photonic bandgap fibers. *Opt Express*. 2012;20(11):12407-12415.
97. Iwama T, Guo Y, Handa S, et al. Thermally-drawn multi-electrode fibers for bipolar electrochemistry and magnified electrochemical imaging. *Adv Mater Technol*. 2021;2101066.
98. Richard I, Schyrr B, Aiassa S, Carrara S, Sorin F. All-in-fiber electrochemical sensing. *ACS Appl Mater Interfaces*. 2021;13(36):43356-43363.
99. Yaman M, Yildirim A, Kanik M, Cinkara TC, Bayindir M. High selectivity Boolean olfaction using Hollow-Core wavelength-scalable Bragg fibers. *Anal Chem*. 2012;84(1):83-90.
100. Yildirim A, Vural M, Yaman M, Bayindir M. Bioinspired optoelectronic nose with nanostructured wavelength-scalable hollow-Core infrared fibers. *Adv Mater*. 2011;23(10):1263-1267.
101. Gumennik A, Stolyarov AM, Schell BR, et al. All-in-fiber chemical sensing. *Adv Mater*. 2012;24(45):6005-6009.
102. Tung N-D, Page AG, Qu Y, Volpi M, Yan W, Sorin F. Multimaterial micro-electromechanical fibers with bendable functional domains. *J Phys D Appl Phys*. 2017;50(14):144001.
103. Qu Y, Tung N-D, Page AG, et al. Superelastic multimaterial electronic and photonic fibers and devices via thermal drawing. *Adv Mater*. 2018;30(27):1707251.
104. Leber A, Dong C, Chandran R, Das Gupta T, Bartolomei N, Sorin F. Soft and stretchable liquid metal transmission lines as distributed probes of multimodal deformations. *Nat Electron*. 2020;3(6):316-326.
105. Du M, Huang L, Zheng J, et al. Flexible fiber probe for efficient neural stimulation and detection. *Adv Sci*. 2020;7(15):2001410.
106. Canales A, Park S, Kilias A, Anikeeva P. Multifunctional fibers as tools for neuroscience and neuroengineering. *Acc Chem Res*. 2018;51(4):829-838.
107. Lu C, Froriep UP, Koppes RA, et al. Polymer fiber probes enable optical control of spinal cord and muscle function in vivo. *Adv Funct Mater*. 2014;24(42):6594-6600.
108. Canales A, Jia X, Froriep UP, et al. Multifunctional fibers for simultaneous optical, electrical and chemical interrogation of neural circuits in vivo. *Nat Biotechnol*. 2015;33(3):277-284.
109. Park S, Guo Y, Jia X, et al. One-step optogenetics with multifunctional flexible polymer fibers. *Nat Neurosci*. 2017;20(4):612-619.
110. Fu R, Luo W, Nazempour R, et al. Implantable and biodegradable poly(L-lactic acid) fibers for optical neural interfaces. *Adv Opt Mater*. 2018;6(3):1700941.
111. Jiang S, Patel DC, Kim J, et al. Spatially expandable fiber-based probes as a multifunctional deep brain interface. *Nat Commun*. 2020;11(1):6115.
112. Lu C, Park S, Richner TJ, et al. Flexible and stretchable nanowire-coated fibers for optoelectronic probing of spinal cord circuits. *Sci Adv*. 2017;3(3):e1600955.
113. Park S, Loke G, Fink Y, Anikeeva P. Flexible fiber-based optoelectronics for neural interfaces. *Chem Soc Rev*. 2019;48(6):1826-1852.
114. Park S, Yuk H, Zhao R, et al. Adaptive and multifunctional hydrogel hybrid probes for long-term sensing and modulation of neural activity. *Nat Commun*. 2021;12(1):3435.
115. Zhang N, Li K, Cui Y, et al. Ultra-sensitive chemical and biological analysis via specialty fibers with built-in microstructured optofluidic channels. *Lab Chip*. 2018;18(4):655-661.
116. Rein M, Favrod VD, Hou C, et al. Diode fibres for fabric-based optical communications. *Nature*. 2018;560(7717):214-218.
117. Zhang T, Li K, Zhang J, et al. High-performance, flexible, and ultralong crystalline thermoelectric fibers. *Nano Energy*. 2017;41:35-42.
118. Maayani S, Foy C, Englund D, Fink Y. Distributed quantum fiber magnetometry. *Laser Photonics Rev*. 2019;13(7):1900075.
119. Shen Y, Wang C, Yang X, et al. New progress on fiber-based thermoelectric materials: performance, device structures and applications. *Materials*. 2021;14(21):6306.
120. Feng Z, Yang S, Jia S, et al. Scalable, washable and lightweight triboelectric-energy-generating fibers by the thermal drawing process for industrial loom weaving. *Nano Energy*. 2020;74:104805.

AUTHOR BIOGRAPHIES

Kaiwei Li received the BE degree in mechanical engineering from Jilin University, Changchun, China, in 2009, and the PhD degree in mechanical engineering from Changchun Institute of Optics, Fine Mechanics and Physics, Chinese Academy of Sciences, Changchun, China, in 2014. He joined the Centre for Optical Fibre Technology, Nanyang Technological University, Singapore as a Research Fellow in 2015. From 2019 to 2021, he was an Associate Professor at the Institute of Photonics Technology, Jinan University, Guangzhou, China. He is currently an Associate Professor at the Key Laboratory of Bionic Engineering Ministry of Education, Jilin University, Changchun, China. His research interests include optic fiber sensors and multimaterial multifunctional fibers.

Lei Wei is an Associate Professor at Nanyang Technological University in Singapore. He received a BE degree from the Wuhan University of Technology in 2005; and a PhD degree from the Technical University of Denmark in 2011. Then he joined the Massachusetts Institute of Technology as a postdoctoral associate. In 2014, he joined the Nanyang Technological University in Singapore as a Nanyang Assistant Professor. In 2019, he was promoted to Associate Professor. He currently serves as the Director of the Centre for Optical Fibre Technology (COFT) at Nanyang Technological University. He also serves as the Chair of The Optical Society (OSA) Singapore Section and the Chair of the IEEE Photonics Society Singapore Chapter. His main research interests are fiber-based devices, multi-functional fibers, bio-fiber interfaces, in-fiber energy generation and storage, and intelligent textiles.

Ting Zhang is currently a Professor at the Institute of Engineering Thermophysics (IET), Chinese Academy of Sciences (CAS), and the Director of the Centre for Advanced Technology at Nanjing Institute of Future Energy System (China). He obtained his PhD degree in Condensed Matter Physics from Beijing Normal University (China) in 2014 and his BE degree in Materials Science and Engineering from Xi'an University of Technology (China) in 2009. He was an Assistant Professor at the Institute of Electrical Engineering, CAS (2014–2015) and a Research Fellow at Nanyang Technological University in Singapore (2015–2019). Professor Ting Zhang specializes in the area of thermoelectrics, hydrogen storage, thermal transport and recovery, and fiber-based devices for energy harvest and storage.

How to cite this article: Shen Y, Wang Z, Wang Z, et al. Thermally drawn multifunctional fibers: Toward the next generation of information technology. *InfoMat*. 2022;4(7):e12318. doi:10.1002/inf2.12318